NORWEGIAN JOURNAL OF GEOLOGY Vol 98 Nr. 4
https://dx.doi.org/10.17850/njg98-4-01

Geological Society of Norway

Integrating subsurface and outcrop data of the Middle Jurassic to Lower Cretaceous Agardhfjellet Formation in central Spitsbergen

Maayke Jaqueline Koevoets[1,2], Øyvind Hammer[1], Snorre Olaussen[2], Kim Senger[2] & Morten Smelror[3]

[1] *Natural History Museum, University of Oslo, P.O. Box 1172 Blindern, 0318 Oslo, Norway.*
[2] *Department of Arctic Geology, University Centre in Svalbard, P.O. Box 156, 9171, Longyearbyen, Norway.*
[3] *Geological Survey of Norway (NGU), P.O. Box 6315 Torgarden, 7491 Trondheim, Norway.*

E-mail corresponding author (Øyvind Hammer): ohammer@nhm.uio.no

The Longyearbyen CO_2 storage project drilling and coring campaign in central Spitsbergen provided new insights on the shale-dominated Middle Jurassic to Lower Cretaceous Agardhfjellet Formation, which is the onshore counterpart to the Fuglen Formation and the prolific source rocks of the Hekkingen Formation in the Barents Sea. Logs of magnetic susceptibility, organic carbon content, organic carbon isotopes and XRF geochemistry on the cores, together with wireline logs, biostratigraphy and sedimentology, have made it possible to refine the interpretation of the depositional environment and to identify transgressive-regressive (TR) sequences. Several key sequence-stratigraphic surfaces are identified and suggested to be correlative in Central Svalbard, and four of them, although not necessarily chronostratigraphic, also to surfaces in the Barents Sea. Due to the nearly flat-lying thrust faults in the upper décollement zone of the West Spitsbergen Fold and Thrust Belt, there is some concern about the lateral correlation of the sequences within Spitsbergen. However, some of the TR sequence surfaces appear to be of regional importance and are recognised both onshore Svalbard and offshore on the Barents Shelf. The observations suggest a shallow-marine shelf depositional environment within an epicontinental sea with variable dysoxic, anoxic and oxic sea-floor conditions. The majority of the facies vary from outer shelf to transition zone or prodelta and lower shoreface/distal delta front. In one outcrop, proximal facies, i.e., delta front or middle shoreface, are recognised. In our study area the nearly 250 m-thick, fine-grained Agardhfjellet Formation is proposed to represent distal shoreline clinoforms and a precursor to the overlying forward- and southward-stepping wedge of the Valanginian Rurikfjellet Formation and the Barremian to Early Aptian Helvetiafjellet Formation.

Keywords: Jurassic, Cretaceous, Agardhfjellet Formation, Svalbard, facies, sequence stratigraphy

Received 14. September 2017 / Accepted 16. January 2018 / Published online 23. March 2018

Introduction

The Agardhfjellet Formation (Middle Jurassic – earliest Cretaceous) in Spitsbergen is predominantly a shale succession with minor siltstones, sandstones and carbonate concretions (Dypvik, 1984b; Steel & Worsley, 1984; Dypvik et al., 1991b; Nagy et al., 2009). Some intervals are enriched in organic carbon and the Agardhfjellet Formation is considered as the lateral time-equivalent of dark shales in the North Sea and Norwegian Sea. In particular, it is regarded as the onshore counterpart to the Fuglen and Hekkingen formations in the Barents Sea. Currently, in the southwestern Barents Sea, the Hekkingen Formation has been proven as the most important source rock (Henriksen et al., 2011). Renewed focus on the oil potential in the southwestern Barents Sea following the Johan Castberg oil discovery

Koevoets, M.J., Hammer, Ø., Olaussen, S., Senger, K. & Smelror, M. 2018: Integrating subsurface and outcrop data of the Middle Jurassic to Lower Cretaceous Agardhfjellet Formation in central Spitsbergen. *Norwegian Journal of Geology 98*, 1–34. https://dx.doi.org/10.17850/njg98-4-01.

has also increased the interest in the onshore equivalent of the Hekkingen Formation.

Core material from shale-dominated cap rock and source rock successions is rare in many basins worldwide (with Western Siberia being a notable exception), and outcrops of shale-dominated successions are commonly weathered and poorly exposed. On Svalbard, the Agardhfjellet Formation is fully cored in four wells drilled near Longyearbyen, representing a unique opportunity for an integrated characterisation of a globally significant succession.

The primary aim of this study has been to document high-resolution biostratigraphy, facies development and sequence stratigraphy of the Agardhfjellet Formation. The formation was previously thought to be the main top seal for potential CO_2 storage in the vicinity of Longyearbyen (Braathen et al., 2012). A large pressure difference between the underlying severely underpressured reservoir and an overlying secondary aquifer testifies to the overall sealing capacity of the Agardhfjellet-Rurikfjellet formations and upper decollement zone (Fig. 1), though it is difficult to exactly pinpoint the main sealing units with the current data. Six wells were drilled within a 50 m radius in Adventdalen 5.5 km southeast of the local coal-fueled power plant, and two wells were drilled near Longyearbyen airport 2 km northwest of Longyearbyen (Braathen et al., 2012). Four of the wells have completely cored the Agardhfjellet Formation, and two of these are also covered by wireline logs, which gives a unique dataset for sedimentological, stratigraphic and geochemical studies.

Geological setting

The study area (Fig. 1) is situated near Longyearbyen in central Spitsbergen, Svalbard. The Svalbard archipelago is located between latitudes 74°–81° north and longitudes 10°–35° east, on the Barents Shelf. The deposits represented in Svalbard range from the Archaean to Quaternary in age (Harland et al., 1997; Dallmann, 1999; Maher, 2001; Worsley, 2008; Henriksen et al., 2011) and were uplifted during the Cenozoic (e.g., Henriksen et al., 2011). The movement along the Hornsund Fault Zone between East Greenland and Svalbard, as a precursor to the opening of the North Atlantic Ocean, initiated the formation of the West Spitsbergen Fold and Thrust Belt (WSFTB) and the associated foreland basin, the Central Tertiary Basin (Eldholm et al., 1987; Braathen et al., 1995; Leever et al., 2011). This episode was dated to 61–62 Ma by Jones et al. (2017). Marshall et al. (2015) concluded that the base of the Paleocene in the Central Tertiary Basin was exposed to a maximum burial temperature of

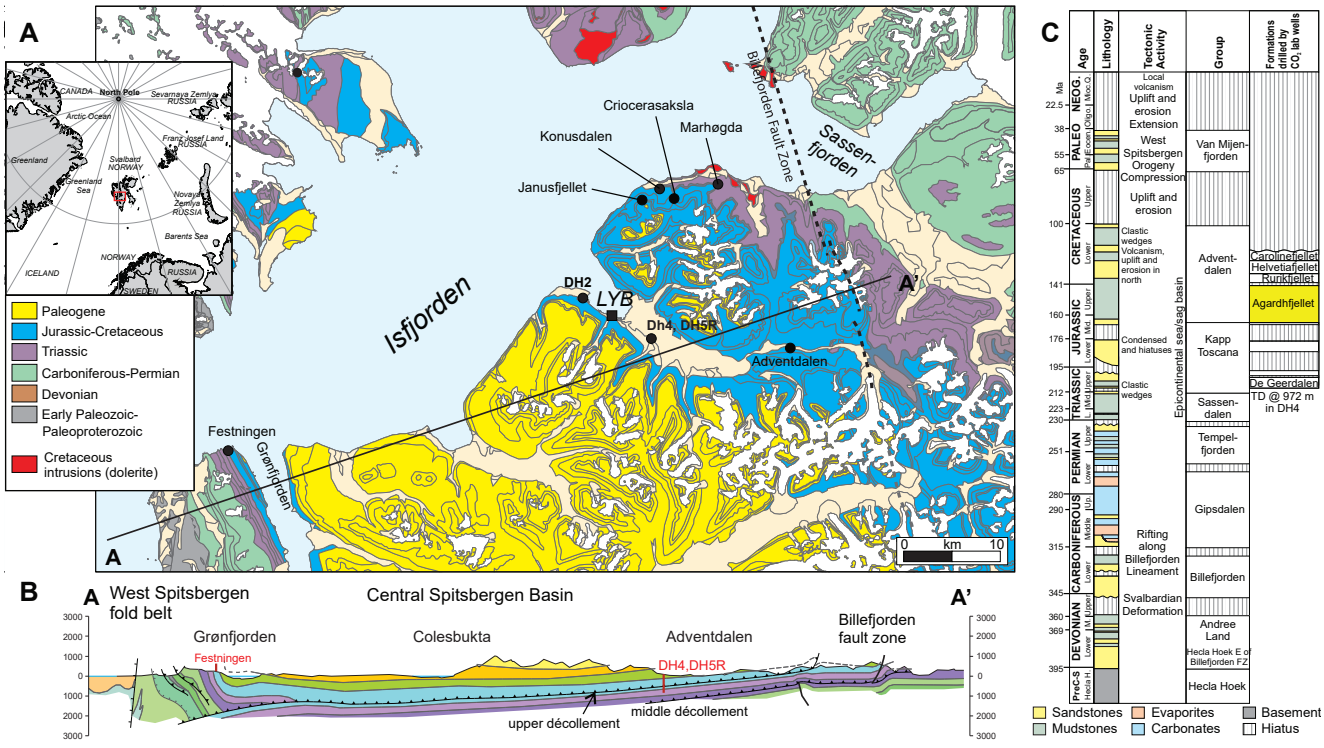

Figure 1. *Geological overview of the study area. (A) Geological map illustrating the location of the DH2 and DH5R/DH4 wells and the outcrops at Janusfjellet, Konusdalen, Crioceraseksla and Adventdalen discussed in the text. Based on Dallmann et al. (2001), digital geological map generously provided by the Norwegian Polar Institute (LYB = Longyearbyen). The inset map shows the location of Svalbard in the North Atlantic. (B) Regional cross-section across the Central Spitsbergen Basin. For location, see Fig. 1A. (C) Regional stratigraphic column highlighting the stratigraphic position of the Agardhfjellet Formation.*

120°C, with a geothermal gradient of 50°C/km. The core material of the Agardhfjellet Formation is approximately 700 m to 1000 m below the base Tertiary unconformity. This would result in a maximum burial temperature of 150°C to 170°C (Marshall et al., 2015). Local heating from Early Cretaceous magmatic intrusions is a common feature in Svalbard (Minakov et al., 2012; Brekke et al., 2014; Senger et al., 2014) but does not seem to have been of regional influence on the Jurassic of the study area (Braathen et al., 2012). Local dykes extending into the Agardhfjellet Formation in the study area (Senger et al., 2013) may locally enhance maturation within the metamorphic aureoles.

The Mesozoic succession in Svalbard is divided into three groups, the Lower–Middle Triassic Sassendalen Group, the Upper Triassic–Middle Jurassic Kapp Toscana Group and the Middle Jurassic–Lower Cretaceous Adventdalen Group. The Triassic deposition across the Barents Sea shelf is mainly characterised by a southeasterly sediment source (i.e., the Ural Mountains, Fennoscandia) with progradation towards the northwest over time, well illustrated by seismic-scale clinoforms across large parts of the Barents Sea shelf (Riis et al., 2008; Glørstad-Clark et al., 2010; Høy & Lundschien, 2011; Anell et al., 2014; Klausen et al., 2015). However, coarse-grained sediment input from the west is reported from the Lower and Middle Triassic in western Spitsbergen. In the Triassic period, most of the sediments originated from a delta-related coastal- and shallow shelf environment, and this trend continued until the Middle Jurassic. Lower to Middle Jurassic, coarse-grained units have so far been the most prolific petroleum reservoirs in the southwestern Barents Sea (Henriksen et al., 2011). Middle Jurassic to lowermost Cretaceous, deeper shelf sediments are found in Svalbard at Hopen, Kong Karls Land, Wilhelmøya, Sørkapp and in the Isfjorden area, while in the Early Cretaceous the shallow shelf shallowed upward to deltaic and flood-plain deposits which were later flooded by Aptian shelf deposits (Dypvik et al., 1991a; Mørk et al., 1999; Krajewski, 2004; Hammer et al., 2012; Midtkandal et al., 2016; Grundvåg et al., 2017). The Middle Jurassic to Lower Cretaceous Janusfjellet Subgroup comprises the Agardhfjellet and Rurikfjellet formations. During the deposition of the Agardhfjellet Formation, shelf conditions were dysoxic to anoxic with periodical oxygenation of the bottom water (Collignon & Hammer, 2012). The Rurikfjellet Formation consists of several coarsening-upward units which were deposited in a marine shelf to prodeltaic and shoreline delta-front environment (Dypvik et al., 1991a, Grundvåg et al., 2017).

The Agardhfjellet Formation is subdivided into four members; in ascending order the Oppdalen, Lardyfjellet, Oppdalssåta and Slottsmøya members (Wierzbowski, 1989; Nagy & Basov, 1998; Mørk et al., 1999; Nagy et al., 2009; Koevoets et al., 2016). The lowermost Oppdalen Member (Bathonian–Oxfordian) is here defined as including the Marhøgda Bed (Bäckström & Nagy, 1985; Krajewski, 1990; Dypvik et al., 1991b). The Oppdalen Member is normally an overall fining-upward unit (Dypvik et al., 1991a). The lowermost part of the Bathonian–Oxfordian Oppdalen Member was deposited in a shallow-marine environment grading into the more distal, black shales of the Lower Kimmeridgian Lardyfjellet Member, which is seen as the lower finer-grained part of a coarsening-upward unit (Dypvik et al., 1991a). A 50 m-thick Upper Kimmeridgian to possibly Lower Volgian coarse-grained siliclastic wedge occurs as the Oppdalssåta Member in our study area. It is organised as 10 – 15 m-thick coarsening-up units and is followed by shales of the Lower Volgian – Ryazanian Slottsmøya Member. The entire Agardhfjellet Formation is up to 250 m thick in our study area, but with considerable lateral variation throughout Spitsbergen, both in total thickness and in the relative thicknesses of its members. Some of this variation is probably linked to tectonic disturbance of the mechanically weak Agardhfjellet Formation in the Cenozoic WSFTB (Braathen et al., 1995; Bergh et al., 1997) which may have resulted in faulted out sections from normal faults or repeated sections from flat-lying ramps/thrust faults (Braathen et al., 1995).

Material and methods

The cores and wireline logs used in this study were obtained by the UNIS CO_2 LAB. The drilling was conducted as part of a project to investigate the feasibility of storing locally produced CO_2 in Upper Triassic–Middle Jurassic naturally fractured sandstones locally on Svalbard (Ogata et al., 2012; Sand et al., 2014). Four of the wells have complete core coverage of the Agardhfjellet Formation (i.e., an average thickness of about 250 m). The successions in the wells were correlated with the classical sections of the Agardhfjellet Formation in the Janusfjellet area, c. 10 km to the northeast of the CO_2 wells (Dypvik et al., 1991a; Mørk et al., 1999; Hammer et al., 2012), as shown in Fig. 2. Depths in wells are reported without correction for regional dip. The wells are located close to the middle of the Central Tertiary Basin syncline in Spitsbergen, and the dip is therefore negligible.

Geophysical logging of the boreholes (Braathen et al., 2012), including natural gamma-ray intensity, formation resistivity and seismic velocity, used slim-hole tools provided by the Geological Survey of Norway (NGU) and Store Norske Spitsbergen Kulkompani (SNSK).

High-resolution sampling for laboratory measurement of magnetic susceptibility is not desirable on valuable core material. Magnetic susceptibility was therefore measured with a Terraplus KT–10 hand-held susceptibility meter at 10 cm intervals from 735 to 510 m in the DH2 core and from 670 m to 435 m in the DH5R core (the interval from 645 m to 651 m was not recovered). The readings

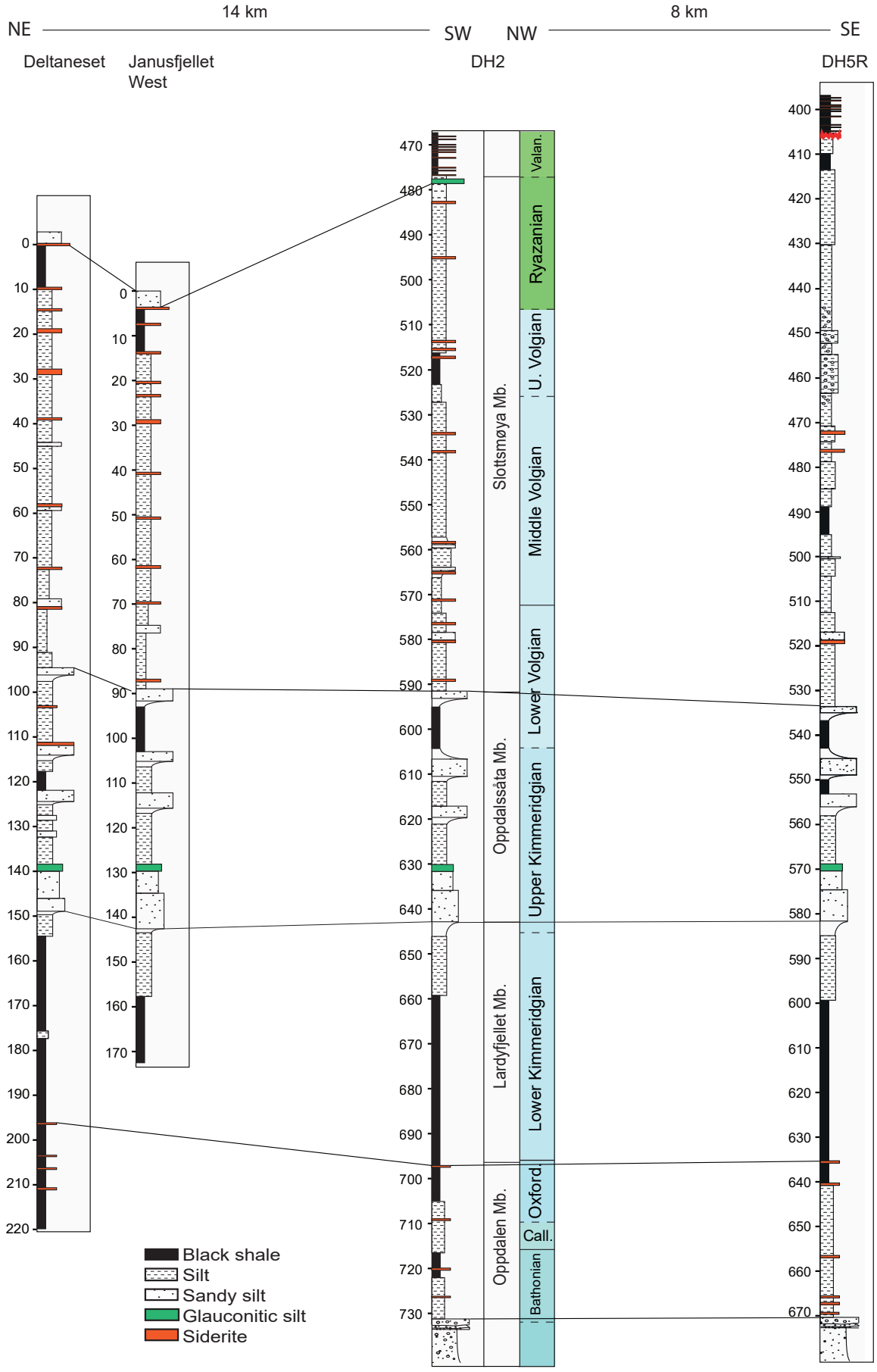

Figure 2. Lithostratigraphic correlation of well and outcrop sections of the Agardhfjellet Formation, Spitsbergen, Svalbard (modified from Koevoets et al., 2016).

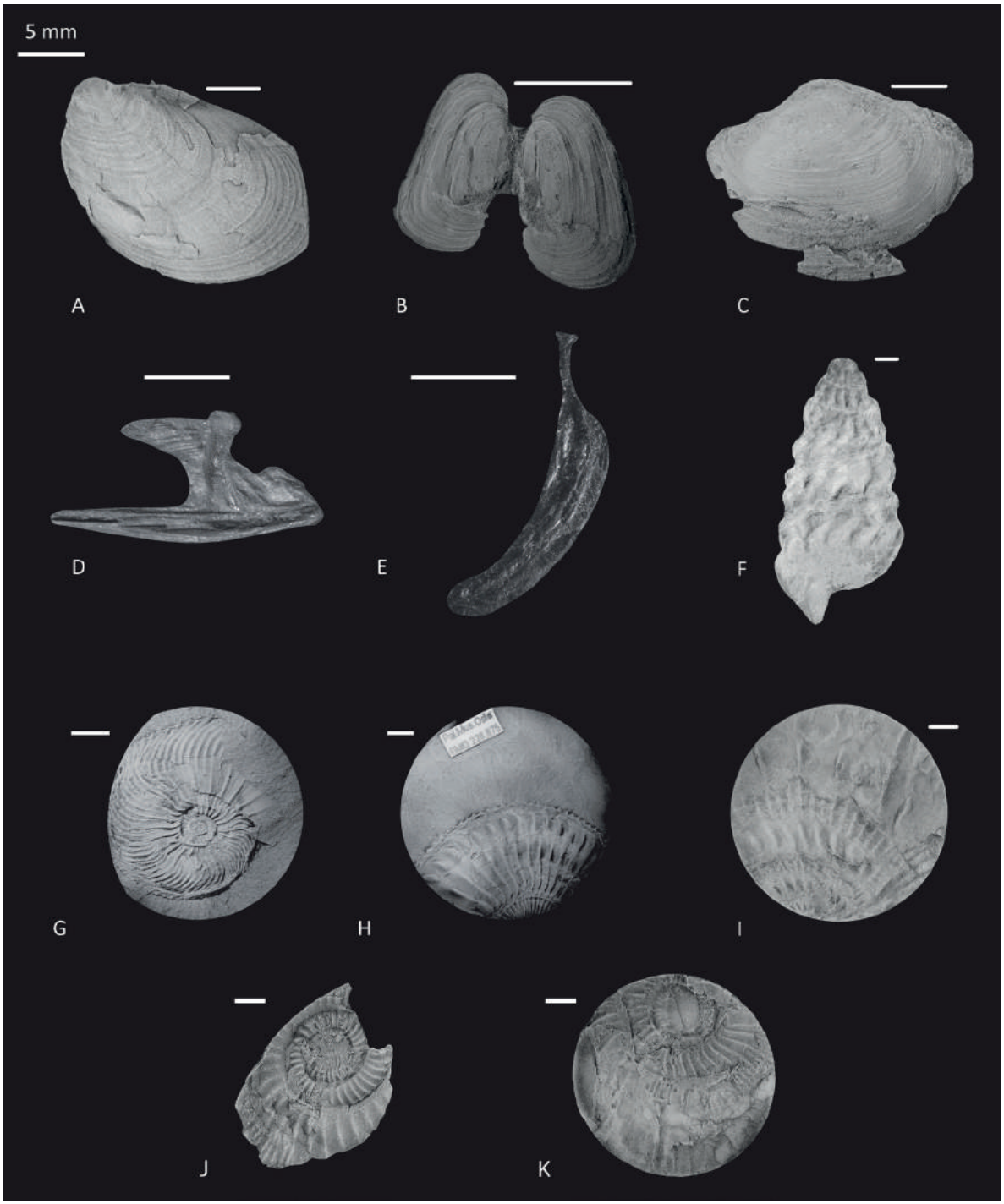

Figure 3. *Typical fossils from the DH2 well. (A)* Buchia *cf.* concentrica*, 663.87 m, Lardyfjellet Member, Lower Kimmeridgian (PMO 228.854). (B)* Grammatodon *sp., 554.44 m, Slottsmøya Member, Middle Volgian (PMO 228.792). (C)* Hartwellia *sp., 601.45 m, Oppdalssåta Member (PMO 228.836). (D)* Leptolepis *cf.* nathorsti*, right dentary of fish, 536.45 m, Slottsmøya Member, Middle Volgian (PMO 228.781). (E)* Leptolepis *cf.* nathorsti*, right maxilla, 677.96 m, Lardyfjellet Member, Lower Kimmeridgian (PMO 228.870). (F) Gastropod, 581.81 m, Slottsmøya Member, Lower Volgian (PMO 228.824). (G)* Cardioceras *sp., 705.9 m, Oppdalen Member, Oxfordian (PMO 228.883, Koevoets et al., 2016). (H)* Amoebites subkitchini*, 693 m, Lardyfjellet Member, Lower Kimmeridgian (PMO 228.875, Koevoets et al., 2016). (I)* Zenostephanus *sp., 645.88 m, Oppdalssåta Member, uppermost Lower Kimmeridgian (PMO 228.847). (J)* Chetaites sibiricus*, 507.95 m, Slottsmøya Member, Lower Ryazanian (PMO 228.753). (K)* Craspedites (Taimyroceras) taimyrensis*, 511.34 m, Upper Volgian (PMO 228.760).*

were corrected for core geometry, the even surface of the core allowing consistent measurements.

Hand-held X-ray fluorescence spectroscopy (HHXRF) used a Thermo Scientific Niton XL3t GOLDD+ instrument with an aperture of 8 mm. Integration time was 90 s in the 'Testall Geo' mode, and measurements were taken at 1 m intervals. After every c. 10 measurements, a calibration measurement was taken on a pressed powder pellet of the USGS Columbia River

Basalt BCR–2 standard, diluted to four parts powder and one part binder. No drift in the measurement of elemental concentrations in the standard was observed. The variance was relatively small, and measurements generally within 10% of the certified standard value (usually much closer). We therefore present uncalibrated curves, which are considered as semiquantitative.

Complete and fragmented macrofossils were noted and counted whenever they occurred on core split surfaces, the density of which was highly variable depending on lithology. A selection of representative fossils is shown in Fig. 3. The main groups noted are ammonites, bivalves and onychites (cephalopod hooks). The presence of other macrofossils such as gastropods, worm tubes, belemnites, wood and fish remains was also marked. A total of 34 samples from borehole DH5R produced foraminifera after standard micropalaeontological processing. A full taxonomic characterisation of the samples was not attempted, but the identified taxa were found at levels in general correspondence with the zonal scheme of Nagy & Basov (1998). Palynomorphs were recovered from 15 samples in borehole DH2.

Lithostratigraphy

The lithostratigraphic subdivision of the members, with the exception of including the Marhøgda Bed into the Oppdalen Member, follows Mørk et al. (1999). The subdivision, in addition to lithology, grain size and sedimentary structures, is based on magnetic susceptibility and wireline logs (Fig. 4). Magnetic susceptibility is generally high in the lower parts of the Lardyfjellet Member, lower in the upper parts of the Lardyfjellet Member and the sandy Oppdalssåta Member, and increasing again in the Slottsmøya Member. Very high susceptibility readings occur at sideritic horizons in the lower (695–730 m in DH2) and upper (520–470 m) parts of the core. Glauconitic horizons at 630 m and 479 m in borehole DH2 also give rise to susceptibility peaks. The other silty and sandy beds generally have low susceptibilities. The transition to the Rurikfjellet Formation in borehole DH2 is characterised by the onset of closely spaced susceptibility peaks due to sideritic nodules.

Gamma radiation reaches maximum values in the dark shales of the Lardyfjellet Member, but is high also in fine-grained intervals of the Slottsmøya Member. P-velocity is generally in opposite phase to gamma radiation, with highest velocities in the well cemented sandstones and siltstones of the Oppdalssåta Member and Slottsmøya Member.

The base of the Agardhfjellet Formation was set at 732 m in borehole DH2 and 671 m in borehole DH5R, at the boundary with the underlying, coarse-grained Wilhelmøya Subgroup (Rismyhr et al., in press). The boundary between the Oppdalen Member and the Lardyfjellet Member is transitional, but was set at c. 630 m in DH5R and 690 m in DH2, near the last siderite bed of the Oppdalen Member and at a reduction in magnetic susceptibility and P-velocity together with an increase in gamma radiation. A coarsening-upwards trend in the Lardyfjellet Member is terminated by the onset of massive sandstones at c. 582 m in borehole DH5R and 643 m in borehole DH2, marking the base of the Oppdalssåta Member. The base of the Slottsmøya Member is also transitional, as thin, silty to sandy beds continue into the lower part of the member.

In borehole DH5R, the succession as observed in borehole DH2 is interrupted by an approximately 20 m-thick diamictite, with the base at around 465 m. In place of the expected upper Slottsmøya Member, in borehole DH5R this interval is characterised by a matrix of claystone with abundant matrix-supported, poorly sorted, subangular to rounded mud clasts and quartz grains. The magnetic susceptibility log is quiet compared to the corresponding interval in borehole DH2, indicating homogenisation of sediment. We interpret this interval as a debris flow, possibly of Late Volgian age. Dinoflagellate cysts above the Slottsmøya Member at 380 m in DH5R indicate a Late Valanginian–Early Hauterivian age (Grundvåg et al., 2017), while an ammonite at 441.8 m is referred to *Laugeites* ex gr. *lambecki* or *Praechetaites* sp., uppermost Middle Volgian *Laugeites groenlandicus* Zone or *Praechetaites exoticus* Zone (M. Rogov, pers. comm., 2014).

The top of the Agardhfjellet Formation was set at 479 m in borehole DH2, at the base of a glauconitic bed which is interpreted as the Myklegardfjellet Bed (Dypvik et al., 1992). The top of the formation was identified at 407 m in borehole DH5R (Mads Engholm Jelby, pers. comm., 2016), about 20 m higher than expected from the succession in borehole DH2, possibly because of the thick diamictic interval (Figs. 2 & 17). The base of the Myklegardfjellet Bed (Birkenmajer, 1980) corresponds to the base of the Lower Cretaceous Rurikfjellet Formation (Mørk et al., 1999). In outcrop it is a 0.5–10 m-thick bed of weathered, plastic clays with dispersed glauconitic grains, interpreted by Dypvik et al. (1992) as alteration products of glauconite. We therefore interpret the 30 cm-thick bed of unaltered glauconitic sandstone at 479 m in borehole DH2 as the Myklegardfjellet Bed, fully confirming that the outcrop expression of this bed is due to a glauconitic horizon.

Chemostratigraphy

Wireline-log characterisation of TOC

The ‘Δ log R’ technique of Passey et al. (1990) was employed to calculate relative organic richness based on a scaled overlay of the sonic and resistivity logs in

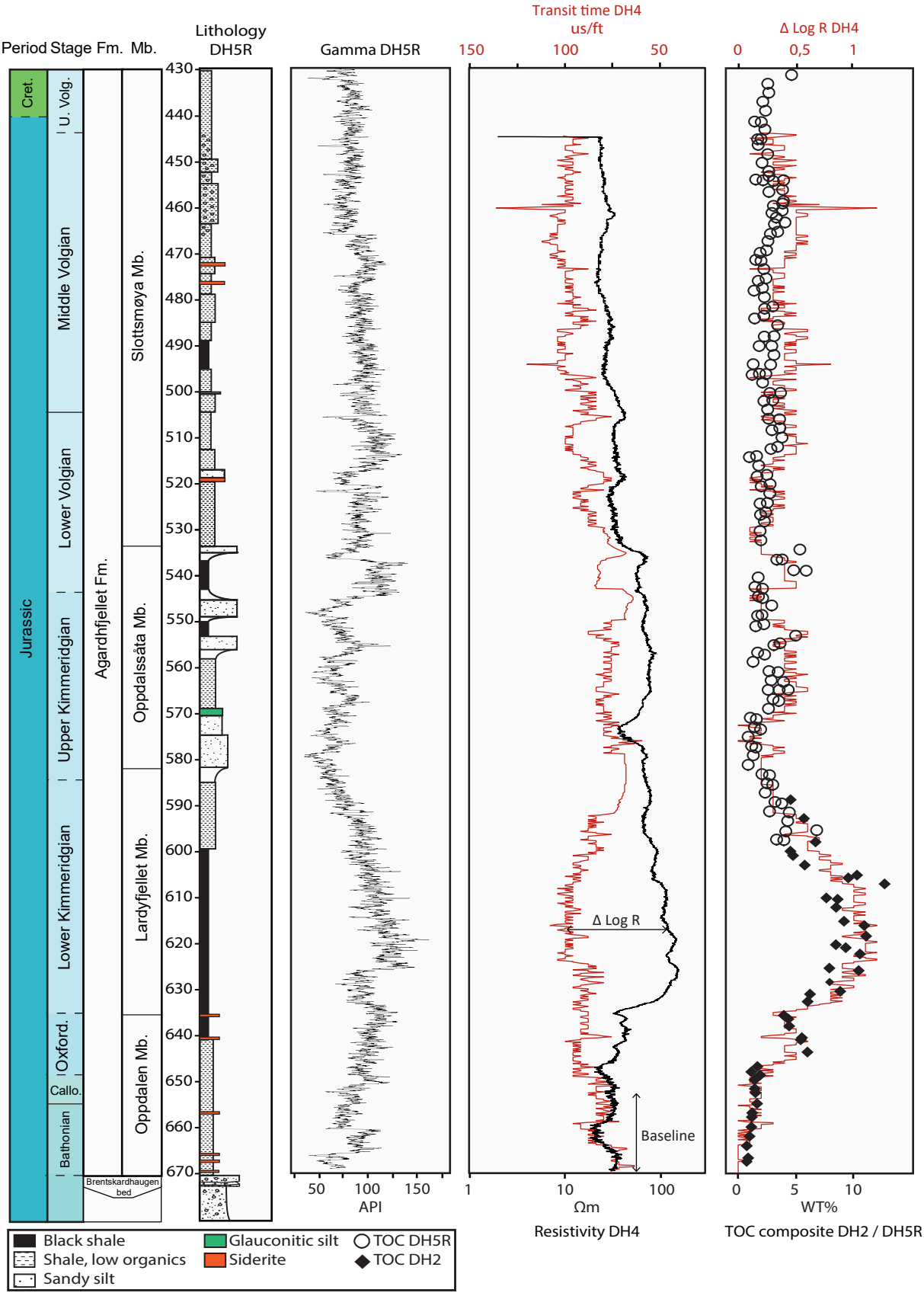

Figure 4. Correlation of wireline data with core-derived TOC values (black circles) following Passey et al. (1990). The Δ log R curve is defined by the separation of scaled resistivity and transit time curves, and provides a qualitative estimate of the TOC. The comparison with the TOC analysed in drillcores by Koevoets et al. (2016) shows remarkable correlation, particularly in the high-TOC interval in the Lardyfjellet Member. For a recent review of the global Jurassic–Cretaceous boundary and its position relative to the Boreal Volgian–Ryazanian boundary, see Shurygin & Dzyuba (2015). Depths are shown for borehole DH5R. Borehole DH4 is very close to DH5R and can be correlated directly, with possible exception for the diamictic interval in borehole DH5R.

borehole DH4 (Fig. 4). The two curves were adjusted to follow each other in the baseline interval from 670 m to 750 m, and the separation was calculated according to:

$$\Delta \log R = \log_{10} (R / R_{baseline}) + 0.02 \times (\Delta t - \Delta t_{baseline}),$$

where Δ log R is the curve separation in logarithmic resistivity cycles, R is the measured resistivity (in Ωm), Δt is the measured transit time (in µsec/ft) and $R_{baseline}$ and $\Delta t_{baseline}$ represent the resistivity and transit time where the curves are baselined (Passey et al., 1990). In this case $R_{baseline}$ = 50 Ωm and $\Delta t_{baseline}$ = 65 µsec/ft.

In intervals with no organic content or hydrocarbons present, both curves will be primarily governed by porosity and thus follow the compaction trend. This is well illustrated in both the upper part of the Agardhfjellet Formation from c. 450–590 m depth and in the underlying reservoir of the Wilhelmøya Subgroup and De Geerdalen Formation from c. 670 m depth. The significant curve separation from 592 to 634 m depth implies the presence of a resistive formation fluid and low-density, low-velocity kerogen. This depth interval correlates precisely with the TOC derived from Rock–Eval evaluation of the drillcores (Figs. 4 & 5).

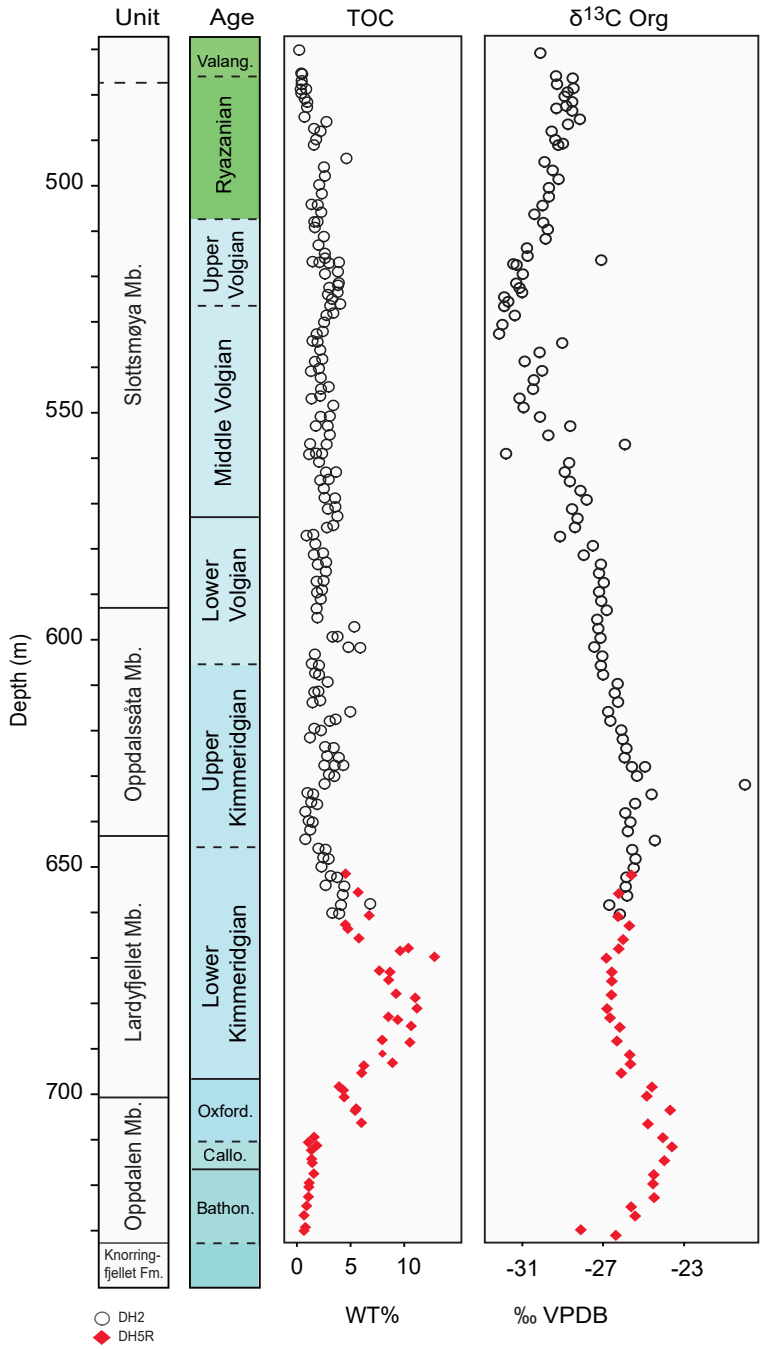

Figure 5. *Composite log of $\delta^{13}C_{org}$ and TOC from the boreholes DH2 and DH5R, after Koevoets et al. (2016). Depths are shown for borehole DH2.*

Stable organic carbon isotopes

Koevoets et al. (2016) presented a high-resolution, composite, organic carbon isotope curve of the Agardhfjellet Formation in the boreholes DH2 and DH5R, with a discussion of its correlation potential. The $\delta^{13}C$ values show a decreasing trend starting from the Callovian/Oxfordian at -24.05‰ to -32.05‰ in the Middle Volgian (Koevoets et al., 2016). Fig. 5 displays the continuous appearance of the organic carbon isotope curve, indicating that the Agardhfjellet Formation in the wells is without hiatuses or repetitions. However, an apparent discontinuity in the TOC values at around 645 m in borehole DH5R (corresponding to 705 m in borehole DH2) may be due to a possible Middle to Upper Oxfordian hiatus in central Spitsbergen, discussed below.

The increase of $\delta^{13}C_{org}$ from the Callovian to the Oxfordian peak (Koevoets et al., 2016) is also recorded on the Isle of Skye, Scotland (Nunn et al., 2009) and in the $\delta^{13}C_{carb}$ in the Atlantic Ocean (Katz et al., 2005) and New Zealand (Podlaha et al., 1998). At the end of the Oxfordian, $\delta^{13}C_{org}$ decreases and remains stable until the Upper Kimmeridgian, after which it continues to decrease towards the minimum value of $\delta^{13}C_{org}$ = -32.05‰ in the Middle Volgian (Koevoets et al., 2016). This Middle Volgian carbon isotope minimum, named VOICE by Hammer et al. (2012), has also been recorded in Scotland (Nunn et al., 2009), Siberia (Zakharov et al., 2014), New Zealand (Podlaha et al., 1998) and the Middle Volga area (Price & Rogov, 2009). The Oxfordian and Volgian carbon isotope excursions thus appear to be useful tools for stratigraphic correlation.

XRF geochemistry

The concentration of some trace elements in shale is influenced by the redox-environment of the water, grain size and other parameters, allowing the concentration or ratio of some elements to be used as palaeoenvironmental proxies (Dypvik, 1984a; Hatch & Leventhal, 1992; Arthur & Sageman, 1994; Jones & Manning, 1994; Powell et al., 2003; Tribovillard et al., 2006; Kylander et al., 2011; Wang et al., 2016). The Zr/Rb ratio, for instance, can be used as a proxy for grain size, as Zr is more prevalent in larger, lithic grains whereas Rb preferably binds to clay particles (Dypvik & Harris, 2001). The Zr/Rb ratio curve follows the lithological observations very well (Fig. 6), and is also comparable with the Zr/Rb curve given by Dypvik & Harris (2001) from the Agardhfjellet Formation at Oppdalssåta. This similarity between the XRF measurements and the stratigraphic log provides a check on the accuracy of the hand-held XRF.

Well known element ratios for bottom-water oxygenation are U/Th and V/(V + Ni) (Hatch & Leventhal, 1992; Arthur & Sageman, 1994; Jones & Manning, 1994; Tribovillard et al., 2006). The concentration of U^{4+} (insoluble) would be enriched over U^{6+} under oxidising conditions (Jones & Manning, 1994). In the same circumstances Th concentrations remain unaffected, allowing for the U/Th ratio to be used as a proxy for oxygenation. Standard values for both these ratios indicating anoxic, dysoxic and oxic environments have all been established (Hatch & Leventhal, 1992; Arthur & Sageman, 1994; Jones & Manning, 1994; Tribovillard et al., 2006).

The V/(V + Ni) ratios indicate that the Oppdalen Member, the Lardyfjellet Member, a small section of the Oppdalssåta Member and the upper part of the Slottsmøya Member were deposited in highly anoxic environments (Fig. 7). However, the U/Th ratios indicate the majority to have been deposited in a dysoxic environment. Cross-plotting these ratios puts most of the Agardhfjellet Formation samples within a dysoxic/anoxic depositional environment (Fig. 7). Also, the XRF sulphur curve (Fig. 6) correlates with some of the inferred low-oxygen intervals, with high values (>10 ppt) through the uppermost Oppdalen Member and the whole of the Lardyfjellet Member (maximum of 38 ppt S at 670 m in borehole DH2).

Biostratigraphy

Ammonites

A number of ammonites were identified in the boreholes DH2 and DH5R (Koevoets et al., 2016), being most abundant in the upper half of the Lardyfjellet Member (Fig. 8). In borehole DH2 an unidentified cardioceratid occurs at 717.7 m. *Kepplerites (Seymourites) svalbardensis* with characteristic triplicate secondary ribs was found at 663.8 m in borehole DH5R (Fig. 8). Kopik & Wierzbowski (1988) found the same species at 4.45 m above the base of the Agardhfjellet Formation at Wimanfjellet (close to Criocerasaksla; Fig. 1) and placed this fauna in the British *Discus* Zone, latest Bathonian (Boreal *Calyx* Zone).

Koevoets et al. (2016) reported *Cardioceras* sp. (earliest Oxfordian) at 705.9 m in borehole DH2. An Early Kimmeridgian ammonite, *Amoebites subkitchini,* was identified at 693 m. This occurrence correlates with the lower part of the *Rasenia cymodoce* Zone (Wierzbowski, 1989). In both boreholes DH2 (660 m to 680 m) and DH5R (609 m to 614 m) an increase in abundance of ammonites is noted in the upper part of the Lardyfjellet Member (Fig. 8). This interval is mainly represented by *Amoebites* sp. of the *kitchini* Zone. Wierzbowski (1989) reported this species from 37.5 m to 48.5 m above the base of the Agardhfjellet Formation at Wimanfjellet, most abundantly in the upper part. In borehole DH2, the interval from 680 m to 667 m contains ammonites with biplicate ribbing, similar to the *Amoeboceras pingueforme* illustrated by Wierzbowski (1989) and triplicate ribbing, similar to the *Rasenia cymodoce* of Wierzbowski (1989),

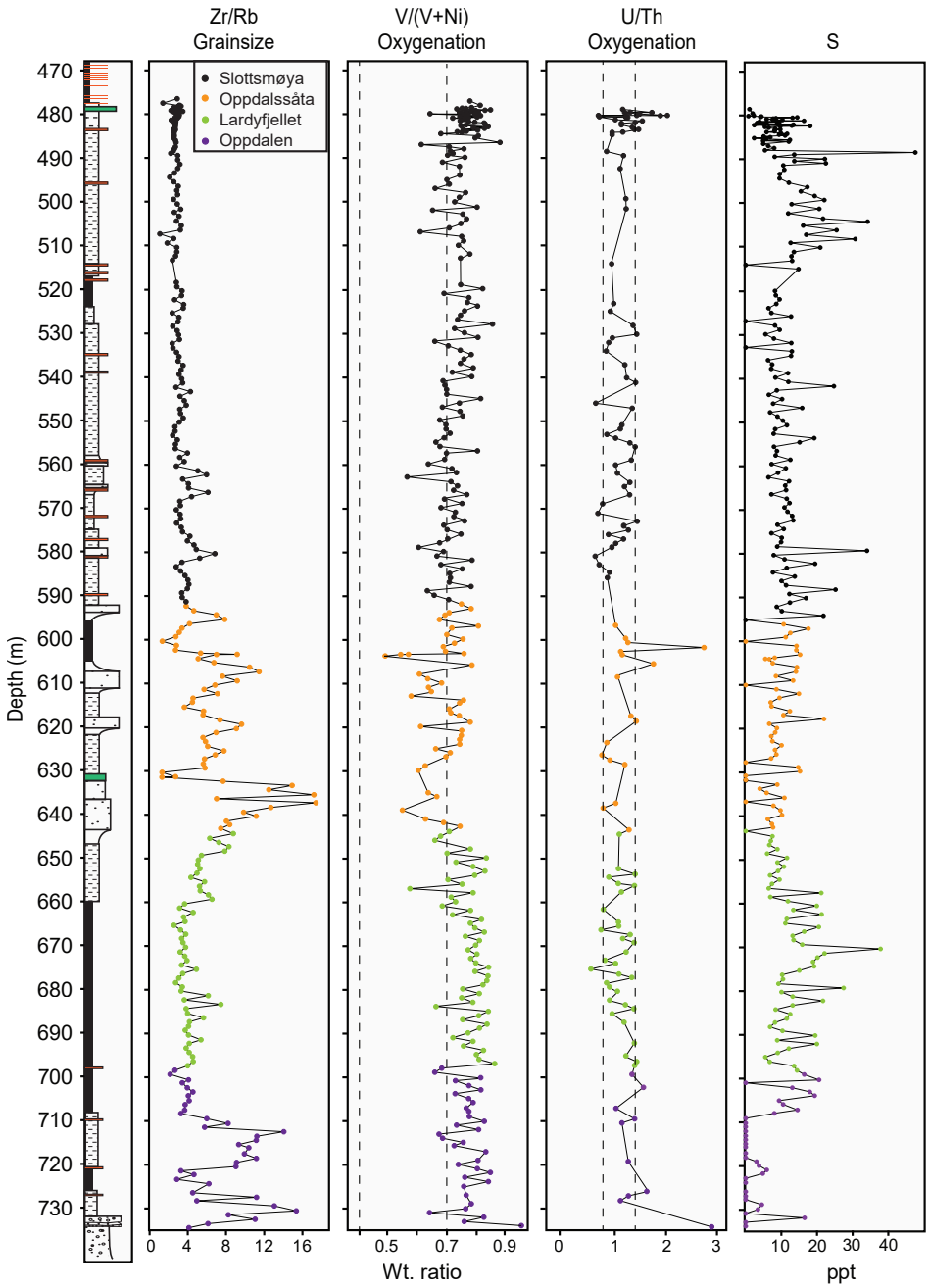

Figure 6. *Stratigraphic profiles of borehole DH2 for trace element redox indices.*

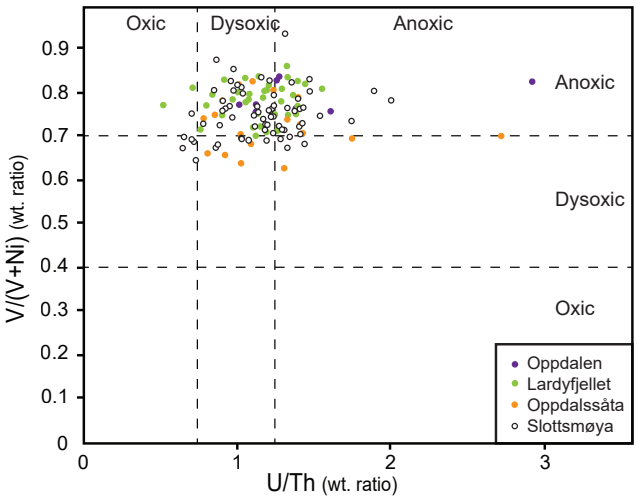

Figure 7. *Crossplot of trace-element ratios used as redox indices of borehole DH2. Ranges for ratios from Hatch & Leventhal (1992) and Jones & Manning (1994).*

i.e., further up in the *Rasenia cymodoce* Zone, Early Kimmeridgian (Wierzbowski, 1989; Rogov, 2014). At 645.9 m in borehole DH2, *Zenostephanus* sp. (Mikhail Rogov, pers. comm., 2017) indicates the very top of the Early Kimmeridgian (Rogov, 2014).

A finely ribbed *Hoplocardioceras elegans* was found at 566.0 m in borehole DH5R, 105 m above the formation base. Wierzbowski (1989) reported this ammonite from 78–80 m above the base at Wimanfjellet. Wierzbowski also mentions glauconitic sandstone 2–3 m below this level, fitting perfectly with prominent green sandstone in the core. The ammonite can be correlated with the upper part of the Late Kimmeridgian *Aulacostephanus eudoxus* Zone of northwest Europe.

Dorsoplanites sp. occurs at 505.6 and 471.9 m in borehole DH5R (Fig. 8). This genus is characteristic of the Middle

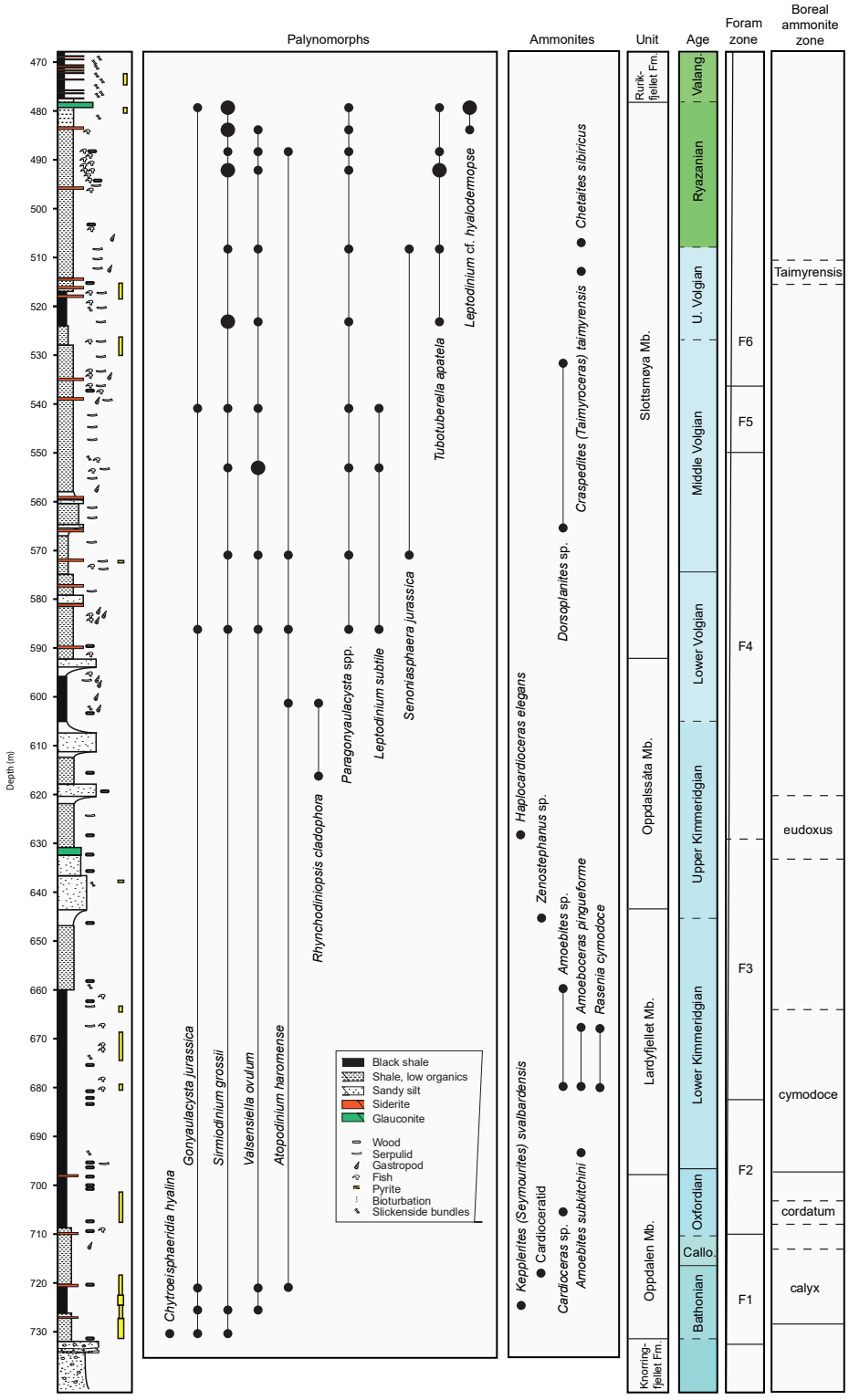

Figure 8. *Dinoflagellate and ammonite occurrences in the Agardhfjellet Formation in borehole DH2.*

Volgian in Spitsbergen (Nagy & Basov, 1998; Rogov, 2010).

At 511 m in borehole DH2, *Craspedites (Taimyroceras) taimyrensis* of the Taimyrensis Zone (Rogov, 2010) was found (M. Rogov, pers. comm., 2017). This genus is characteristic for the Upper Volgian of the Arctic. At 507 m in borehole DH2 an ammonite probably belonging to *Chetaites sibiricus*, lowermost Ryazanian, has also been observed (M. Rogov, pers. comm., 2017).

Dinoflagellate cysts

The abundance of palynomorphs through the Agardhfjellet Formation in central Spitsbergen varies considerably and the preservation is generally rather poor (Bjærke, 1980; Århus, 1988; Dalseg et al., 2016a). Best recoveries of marine palynomorphs are in the Oppdalen Member and Slottsmøya Member, while the four samples included from the Lardyfjellet Member are barren (Fig. 8).

The presence of the dinoflagellate cysts *Chytroeisphaeridia hyalina* and *Sirmiodinium grossii* at 730.20 m suggest a correlation to the Late Bathonian – earliest Callovian *Sirmiodinium grossii* concurrent range zone in the Barents Sea Region as defined by Smelror & Below (1992). According to Riding & Thomas (1992), *S. grossii* first appear in the *Discus* ammonite zone in the British Jurassic, and the ammonite fauna recovered at 717.7 m in borehole DH2 supports a correlation to this zone. In East Greenland, the oldest appearance of *S. grossii* correlates to the Late Bathonian *Calyx* ammonite zone (Smelror, 1988a). An age not younger than Bathonian for the lower Oppdalen Member is supported by the recovery of *Valvaeodinium spinosum* at 730.20 m, as this species is reported to have its last appearance datum in the Late Bathonian of Subboreal Northwest Europe (Poulsen & Riding, 2003).

A dinoflagellate cyst assemblage with *Energlynia acollaris*, *Evansia evittii*, *Fromea tornatilis*, *Gonyaulacysta jurassica* and *Mendicodinium groenlandicum* was recovered at 724.50 m. This correlates to comparable assemblages recovered in the Bathonian and lowermost Callovian on Kong Karls Land, eastern Svalbard (Smelror, 1988b).

No age-diagnostic marine palynomorphs were found in the samples from the upper Oppdalen Member (700.20 m), in the Lardyfjellet Member (samples from 689.95 m to 650.47 m) or in the lower-middle Oppdalssåta Member (638.48 m and 632.47 m). The recovery of *Atopodinium haromense*, *Cribroperidinium* spp. and *Rhyncodiniopsis cladophora* at 616.50 m may suggest a rough correlation to the Kimmeridgian *Rhynchodiniopsis cladophora* (Rc) dinoflagellate cyst zone as defined in West Siberia by Ilyina et al. (2005), although these taxa are also known from older Upper Jurassic strata.

The dinoflagellate cyst assemblages found in the Slottsmøya Member support a Volgian age for the upper part of the Agardhfjellet Formation. Characteristic species are *Cribroperidinium* spp., *Paragonyaulacysta* spp. (FAD at 586.50 m), together with common to abundant *Sirmiodinium grossii* and *Valensiella ovulum*. Århus (1988) reported an acme of *Valensiella ovulum* at 170 m above the base of the Agardhfjellet Formation at Janusfjellet. This corresponds with beds containing *Isocyprina inconspicua* and *Isocrinus* sp. and about 1.5 m below the lowermost/oldest records of *Dorsoplanites* sp.. A comparable acme is recorded at 540.49 m in DH2, suggesting a latest Early or Middle Volgian age at this level.

Dalseg et al. (2016b) defined two informal dinoflagellate cyst zones 1 and 2 in the Slottsmøya Member at Janusfjellet and Knorringfjellet in central Spitsbergen. In borehole DH2, the boundary between the zones is recognised at 552.57 m by the last abundant occurrence of *Paragonyaulacysta* spp. and the first common occurrence of *Tubotuberella apatela.*

The youngest occurrences of *Leptodinium subtile* at 540.49 m and *Senoniasphaera jurassica* at 508.32 m suggest a Middle Volgian age at this level, i.e., dinoflagellate cyst zones DSJ35–37 of Poulsen & Riding (2003). However, these species may also have been reworked, as also reworked Kimmeridgian dinoflagellate cyst species (i.e., *Subtilisphaera? paeminosa, S. inaffecta*) are found in the upper part of the Slottsmøya Member.

The presence of *Leptodinium* cf. *hyalodermopse* at 483.50 m and 479.50 m in borehole DH2 could also be of stratigraphic significance. Århus (1988) recorded the earliest appearance of this species, together with *Cribroperidinium ehrenbergii*, *Paragonyaulacysta* spp. and *Gonyaulacysta helicoidea*, in the Ryazanian of the Janusfjellet section. The presence of *Cribroperidinium ehrenbergii*, *C. sarjeanti* and *Paragonyaulacysta* spp. at 479.50 m may, however, favour a somewhat older age, as these species are typically more common in the Volgian than in the Ryazanian.

Renewed analysis by Aptec from borehole DH5R confirms that there are very few or no age-diagnostic dinoflagellate cysts in the Lardyfjellet Member and Oppdalssåta Member. Of interest is the total dominance of the freshwater alga *Botryococcus* in samples 624.65 m (Lardyfjellet Member) and 420.5 m (Oppdalssåta Member).

Other invertebrate fauna

Hydrocarbon seep deposits of the uppermost Agardhfjellet Formation have revealed over 17 species of bivalves and a number of other invertebrates (Hryniewicz et al., 2014). The invertebrate remains recovered from the shales and siltstones in the outcrop

are fragmented due to frost wedging, and macrofossils can be difficult to recover. Birkenmajer et al. (1982) recorded identifiable macrofossils from only eight horizons. The core material proved to contain a more continuous record of the invertebrate fauna. Borehole DH5R contains abundant and well preserved moulds of invertebrates. A more detailed study of the DH2 core revealed that the Agardhfjellet Formation contains a far more abundant bivalve fauna than previously assumed. Where the Oppdalen, Lardyfjellet and Oppdalssåta members have a sparse distribution of bivalves, the Slottsmøya Member contains a greater amount than the previous three members combined.

No identification of bivalves was conducted. However, at 500 m in borehole DH2 there is a sudden decline in bivalve abundance. This point coincides with strong increase in onychite (Hammer et al., 2013) abundance. At 485 m in borehole DH2 the onychites disappear for a few metres and lingulid brachiopods dominate. The lingulids show strong resemblance to the *Lingularia* from the lowermost Cretaceous hydrocarbon seeps on Spitsbergen (Holmer & Nakrem, 2012) and also described from the Volgian of Western Siberia (Smirnova et al., 2015). The occurrence of the brachiopods in borehole DH2 is close to the seep interval (Hammer et al., 2011) and further examination will determine if they belong to the same species. These changes are sudden and can indicate an abrupt change in depositional environment.

Marine reptiles

The Slottsmøya Member is well known for the presence of ichthyosaur and plesiosaur remains and their exceptional three-dimensional preservation (Druckenmiller et al., 2012; Hurum et al., 2012; Knutsen et al., 2012; Delsett et al., 2016, 2017). The abundance of the marine reptiles is highest in the Middle Volgian and coincides with a strong increase in abundance of bivalves (Delsett et al., 2016).

Facies and facies associations

Based on lithology, sedimentary and biogenic structures, fossils and chemical analysis, the succession has been subdivided into eight facies, F1–8, as summarised in Table 1.

These facies are grouped into four facies associations, FA 1 to FA 4 (Table 2). Detailed sedimentological logs from fully cored successions and wireline logs supported by outcrop photos illustrate the different facies and facies associations (Figs. 9–15). While all facies associations are recognised in both outcrop and wells, some of the individual facies are only recognised in wells and not in outcrops, and vice versa. The local occurrence of F8 (authigenic carbonate in hydrocarbon paleoseeps) in the Janusfjellet section (Hammer et al., 2011), for example, is not recognised in the wells. The diamictite, F5, seen in the Slottsmøya Member in borehole DH5R, is not observed in outcrops. This might be a more common facies in the Agardhfjellet Formation in central Spitsbergen, but probably missed here due to weathered outcrops.

FA 1: Outer-shelf mud deposits

Description: FA 1 is the dominant facies association in the Agardhfjellet Formation and consists of facies F1 comprising black, millimetre-laminated, organic-rich shales i.e., 'paper shales' (Fig. 9), and F2, laminated, dark grey to black, silty shale with up to 40% silt. Abundant beds or laminae rich in bivalves or fish remains are observed in some places in F2. Pyrite is common together with ankerite/dolomite and siderite concretions (F7) that are often stratiform. Thin laminae (Fig. 9A) of very fine-grained sandstone or siltstone are intersecting both F1 and F2. FA 1 varies from a few metres to tens of metres thick tabular successions. In the Lardyfjellet Member it forms a part of a fining-upward (FU) unit from FA 3 and transitions into the basal part of an overlying coarsening-upward (CU) unit of the transition zone/pro delta facies association, FA 3 (Fig. 12). A sharp boundary is commonly observed between F1 and F2. The offshore marine, condensed facies association, FA 2, is in places embedded in FA 1. Collignon & Hammer (2012) described the dark-grey silty shale, F2, to be blocky and prismatic with occurrences of thin silt- to sandstone beds and carbonate concretions. Geochemical analyses of F1 in the transition zone between the Oppdalen Member and the Lardyfjellet Member have shown TOC values up to nearly 12.8% (Koevoets et al., 2016). XRF results show low Zr/Rb ratios (typically around 4) in FA 1 but higher values in FA 2 (Fig. 6). V/(V + Ni) ratios are high, typically above 0.7, while the S content is variable but generally highest in the FA 1 of the Lardyfjellet Member and the upper part of the Slottsmøya Member (Fig. 6).

Bioturbation is scarce in F1 and F2 and has a BI index of 0–3 with common, small *Palaeophycus* and thin tubes of *Skolithos* and *Aulichnites* burrows. Ammonites, belemnites, bivalves, gastropods, fish, crinoids, ophiurids, asteroids (Rousseau & Nakrem, 2012), abundant polychaete tubes, onychites (Hammer et al., 2013), brachiopods and marine reptiles are the observed macrofossils in this facies association. At some levels, the abundance of bivalves and fish skull remains can justify the terminology bivalve and fish shales, respectively. Nagy et al. (1990) reported laminae/beds of 'foraminifer sandstone' in the upper part of the Oppdalssåta Member and Slottsmøya Member in central Spitsbergen. Within this facies association, fossiliferous methane seep carbonates F8 occur in nearby outcrops at Janusfjellet (Hammer et al., 2011). In contrast to carbonates or carbonate-cemented sandstone/siltstone, it consists of

Table 1. *Facies occurring in the Agardhfjellet Formation .*

Facies	Description	Ichnology BI = Bioturbation Index	Interpretation
F1. Paper shales	Black, in places weathering bluish organic-rich paper shale with mm-thick laminae of siltstone and shale. Common ammonite and belemnite fossils, bivalves and gastropods are present. A few trace fossils were found. Pyrite and pyritisation of fossils are present in some layers.	BI = 0–1. Low diversity, monospecific ichnofossil assemblage. Small *Palaeophycus* are most common.	High organic productivity in a stratified saline water mass. Deposited below storm wave base, distal from sediment input and probably mostly clay fallout from hypopycnal flow. Anoxic to dysoxic bottom water.
F2. Dark grey silty shales	Laminated dark-grey to grey shale with a high silt component (~20 – 40 %). Common pyritisation. Diverse invertebrate and vertebrate fossils are present in varying abundances.	BI = 0–3. Varying low- to high-diversity ichnofossil assemblages. *Palaeophycus*, thin *Skolithos*, *Chondrites* and *Aulichnites*.	Deposited below storm wave base, more proximal to sediment input than F1, i.e., higher sedimentation rate. Mostly deposited from mixture of hypopycnal and hyperpycnal flow. Oxic to dysoxic bottom water.
F3. Heteroliths	Dark-grey, faintly bedded, very fine-grained sandstones. Commonly completely burrowed. In places intersected by hummocky cross-stratified sandstone beds. Rare laminated and rippled sandstone.	BI = 3–5. *Palaeophycus*, small *Chondrites*.	Deposited near storm wave base, mostly from hyperpycnal flow.
F4. Sandstones	Light- to dark-grey coloured, very fine- to fine-grained sandstones. Thickness varies from 0.1 to 3 m. Varies from burrowed to homogenous sandstone beds. Main sedimentary structures are hummocky cross-stratification, wave and current ripples, lamination and rare dunes. Commonly carbonate cemented. Gastropods are common in some layers. Scattered glauconitic grains.	BI = 3–4. *Skolithos, Thalassinoides, Teichichnus, Palaeophycus*, small *Chondrites*, *Arenocolites, Planolites* and *Rhizocorallium*.	Deposited by oscillation and traction flow between fair weather and storm wave base. Oxygenated bottom waters.
F5. Diamictite	Matrix-supported mudstone conglomerate or diamictite. Sub-angular to rounded sandstone clasts. Mudstone rip-up clasts occur together with laminated convolute bedding. A single bivalve and a single crinoid stem section embedded in the diamictite.	BI = 0–1. *Chondrites, Planolites* and *Nereites*.	Non-Newtonian flow – cohesive debris flow. Deposited in a slope environment below storm wave base.
F6. Glaucony to glauconitic sandstone/ shale	Fine- to medium-grained sandstone up to 0.5 m and thick siltstone/shale. Weathers reddish while some beds weather into a green unconsolidated clay, i.e., Myklegardfjellet and Marhøgda Bed.	BI = 1–5. *Trichichnus*.	Formed near the sediment water surface over long periods of time. Typically develops in areas of low sediment input. Commonly transgressive and in outer marine shelf, distal to deltaic or fluvial input.
F7. Carbonates	From clean to sandy or muddy siderite or dolomite/ ankerite, rare calcite. Beds or concretions, commonly with glauconite grains and rare chamosite ooids. Concretions are mostly stratiform. Bedded units may reach up to 1 m in thickness. Bivalves and gastropods, with a few ammonites and belemnites occur on top surfaces in some of these beds. Packed bed with ammonites, bivalves, belemnites and scattered vertebrate bones, wood fragments and crinoids (e.g. the informal Dorsoplanites bed) is classified as coquina. Phosphate grains.	BI = 2 – 4. *Chondrites*.	The beds are deposited with no or very slow allochthonous sedimentation, i.e., condensed. Near storm wave base. Coquinas suggest storm beds but well-preserved fossils indicate a more distal setting. High productivity of benthic and nektonic fossils. Dolomite; originally open marine, oxic sea floor and water column. Siderite might reflect mixed sea bottom conditions.
F8. Authigenic carbonate in hydrocarbon palaeoseeps.	Very large (>1m) rubbly concretions. Complex microfacies reflect several generations of precipitation and brecciation with abundant bioclasts and macrofossils. Botryoidal, zoned calcite growth textures and primary voids filled with late diagenetic sparite. The calcite cement has light carbon isotopic composition. Abundant, well-preserved bivalves, brachiopods, ammonites, belemnites, gastropods, foraminifera, tubeworms and wood fragments. Hydrocarbon stained. For detailed description see Hammer et al. (2011) and Hryniewicz et al. (2012).	Small, hard ground boring	Authigenic formation of carbonates in a hydrocarbon palaeoseep environment.

Table 2. *Facies associations of the Agardhfjellet Formation.*

Facies association	Facies geometries and thickness	Interpretation
FA 1	Up to 60 to 70 m-thick tabular successions. Consists of F1, F2 and rare F8.	Outer shelf with variable high to low organic mud deposits. Variable oxic, dysoxic and anoxic sea-floor conditions. Represent toe sets of clinoforms.
FA 2	Facies F6, F7. Up to 1 m-thick beds.	Inner to outer shelf marine condensed deposits. Either toe sets or foresets of clinoforms.
FA 3	Up to 20 m-thick tabular successions and consist of F3, F4 and F5. Part of CU or FU units	Transition zone/prodelta. slope set of clinoforms
FA 4	Facies F3, F4. Up to 10 m-thick tabular sandstone bodies. Commonly seen in upper part of CU units. Also observed as lateral pinching out to shale.	Lower middle shoreface or delta front. Foreset rollover position of clinoforms.

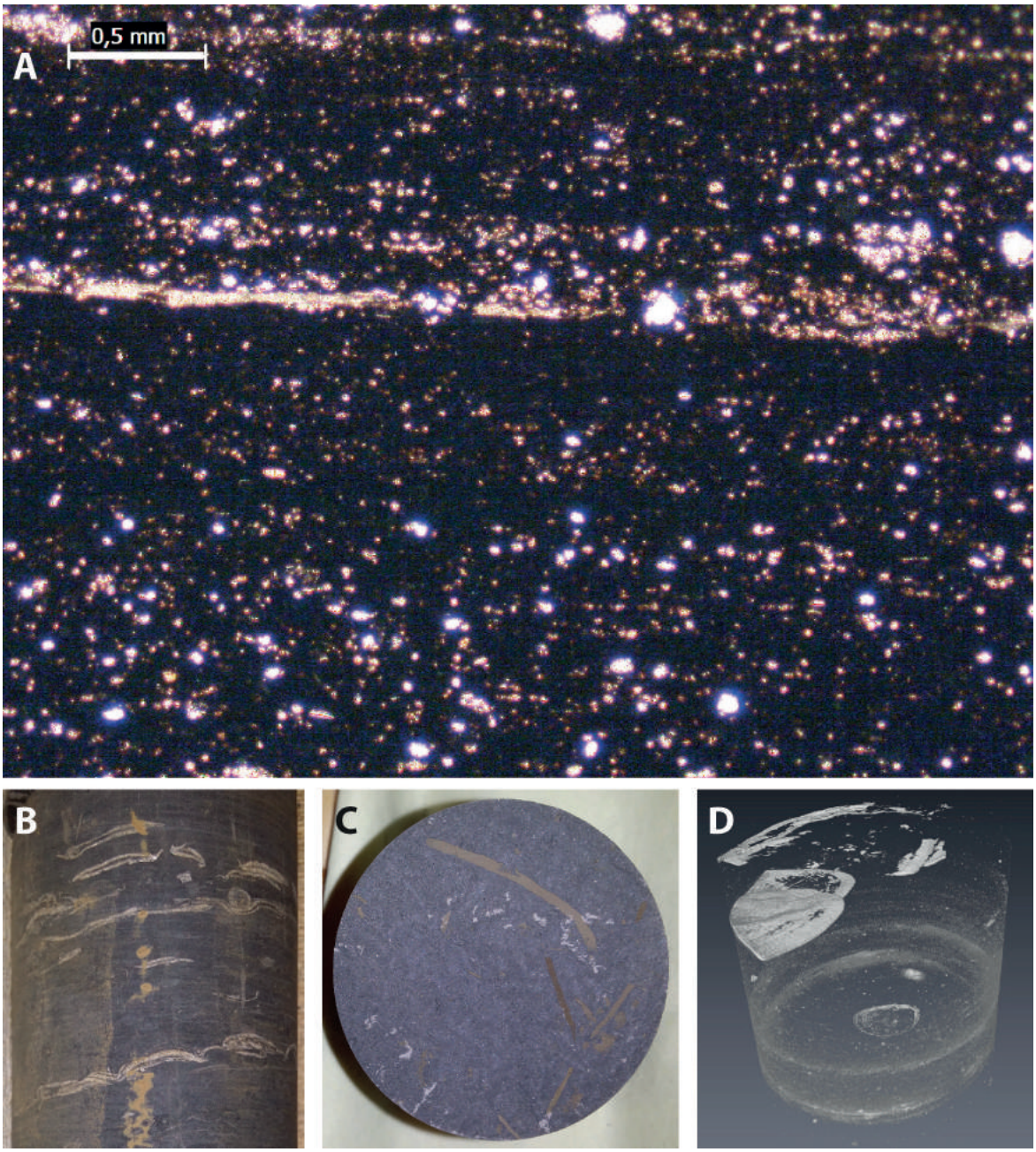

Figure 9. *(A) Microscope image of thin-section at level 666 m in DH2, showing thin laminated shale, F1. (B) Multiple invertebrate specimens in the Slottsmøya Member at 508.80 m. (C) Cross-section of well DH2 at 509.60 m with visible shallow burrows. (D) CT-scan image of bivalves at 671.51 m; the pyritisation of these specimens allows for some details of shell structure to be recognised. Core diameter is 5 cm.*

calcite and has a very rich fauna with well-preserved fossils. In Agardhbukta, East Spitsbergen, in the same stratigraphic level, five multi-storey similar carbonate bodies are also embedded in FA 1 (Abay et al., 2017). The gamma log shows cylinder (block) and serrated to smooth traces. High-velocity log spikes represent carbonate beds or concretions from FA 2. Sideritic beds or concretions give high spikes in the magnetic susceptibility log.

Interpretation: Hvoslef et al. (1986), Koevoets et al. (2016) and Abay et al. (2017) showed that the paper shale in the Agardhfjellet Formation (F1) has a high HI index (236 mg HC/g organic C) and TOC values of up to 12.8%. This, together with the absent or sparse trace fossils and benthic invertebrate fossils, suggests anoxic sea-floor conditions. The more burrowed shales of F2 with invertebrate fossils and lower TOC values up to 4% suggest dysoxic conditions. This interpretation is supported by V/(V + Ni) ratios. As discussed below, the presence of siderite rather than calcite cannot be used to infer sea-floor oxygenation directly, as these siderite concretions most likely formed at great burial depths in the Agardhfjellet Formation (Krajewski, 2004). A lack of wave structures in the sporadic, thin, very fine-grained sandstone laminae indicates deposition below the storm wave base on a mud-dominated shelf. The shale has either settled from suspension under low energy conditions or alternatively by higher energy, dense suspension flows (e.g., Macquaker et al., 2010). In a study of the similar organic-rich Kimmeridge Clay Formation in the U.K., Macquaker & Gawthorpe (1993) showed that the black, silt-rich shale (like F2) was deposited at a proximal shallow shelf position near the storm wave base under a high sedimentation rate. The dominance of kerogen type III in F2 is consistent with this interpretation. The black, organic-rich, laminated shale (similar in description to our F1) was deposited in a more distal location, still close to the sediment source. Macquaker & Gawthorpe (1993) interpreted the deposition as representing an outer shelf environment and with a stratified water column with high organic productivity in the uppermost layers, partly controlled by an incoming freshwater discharge. Based on the foraminiferal assemblages, Nagy et al. (2009) concluded that 'salinity'-induced stratification of the water mass was an important factor during deposition of the muds in the Agardhfjellet Formation. Some of the black paper shale, F1, in the upper part of the Slottsmøya Member is devoid of bivalves but contains many onychites and teleost remains, consistent with a stratified water column, i.e., an oxygenated water layer overlying anoxic bottom waters. Also, the common occurrence of the fresh/brackish water alga *Botryococcus* together with ammonites and belemnites points to a stratified water column.

The highest TOC values as seen in the lower part of the Lardyfjellet Member which constitutes the lower part of the large-scale coarsening-upward trend from prodelta (FA 3) to distal delta front (FA 4), suggest the possibility of an influx of freshwater plumes with nutrients and perhaps blooming of algae. The fauna in the carbonate methane seeps suggest deposition below storm wave base and probably at around 100 m water depth (Hryniewicz et al., 2015). Although subtle, FA 1 in the Slottsmøya Member is often overlain by a coarsening-upward unit (Dypvik & Zakharov, 2012; Hammer et al., 2012). Here, the CU units shallow upward to the transition zone or prodelta facies association, FA 3. The thin laminae (Fig. 9) of siltstone and very fine-grained sandstone seen in FA 1 might represent either distal storm beds or deposits from hyperpycnal flows resulting from nearby fluvial input. Occurrence of fossiliferous laminae in FA 1 may also either represent distal storm beds or a temporary change in oxic, dysoxic and anoxic conditions. Some foraminifers identified by F. Gradstein in Hammer et al. (2012) suggest an inner shelf to offshore transition zone also in the Slottsmøya Member. The fish and bivalve shales and 'foraminifer sandstone' are suggested to represent sorting by winnowing of clay/silt by sea bottom currents. Sharp-based, hummocky cross-stratified beds (Fig. 14) resting on the black paper shale of FA 1 suggest storm deposits, i.e., tempestites, in an offshore or transition zone.

We conclude that FA 1 was deposited in a shallow outer-shelf environment probably close to the storm wave base and under variable oxic, dysoxic and anoxic sea-floor conditions. We favour the conceptual model by Macquaker & Gawthorpe (1993) that the black organic-rich shales of F1 represent a low sedimentation rate with high organic production in a salinity-stratified water column with anoxic to dysoxic sea floor in a shelf environment. F2 represents higher sedimentation rates in a more proximal position, with more burrows suggesting oxic or at least periodic anoxic-oxic sea-floor conditions. These interpretations are in general agreement with previous studies which have suggested that the shales were deposited on the outer shelf (Dypvik et al., 1991b; Krajewski, 2004; Nagy et al., 2009). FA 1 is commonly seen at the base of a prograding unit (CU unit), and then the sharp boundary observed in places between F1 and F2 suggests a sudden shift in sedimentation rate due to delta shift, i.e., avulsion or a sudden change in base line.

FA 2: Offshore marine condensed deposits

Description: This facies association is scattered throughout the formation and consists of two facies: F6 glauconitic sandstone and F7 carbonates. In places, the carbonates contain well preserved invertebrates with calcite shells. Bäckström & Nagy (1985) described a 1.5 m-thick, tabular, condensed unit, i.e., the Marhøgda Bed, in nearby outcrops at Marhøgda, northeast of Konusdalen. It occurs in the lower part of the Oppdalen Member and in our study we define it as the basal part of the Agardhfjellet Formation. At Marhøgda it shows an

unconsolidated, 20 cm-thick, glauconitic sandstone (F6) resting on the top surface of the Brentskardhaugen Bed, followed by a 20–30 cm-thick monomict conglomerate with well-rounded phosphate pebbles. At the base of the Marhøgda Bed, i.e., top surface of the Brentskardhaugen Bed, Krajewski (1990) observed stromatolites and encrusting agglutinated foraminifera in Van Keulenfjorden, south of our study area. The succession is capped by an up to 1 m-thick dolomite mudstone bed (F7) containing allochems of rare quartz and chert grains, scattered chamosite ooids, and phosphatic and glauconite grains. In DH5R, above the Brentskardhaugen Bed, FA 2 consists of dark-grey greenish carbonate with floating, coarse to very coarse quartz and glauconite grains, suggesting a somewhat similar development. F7 is a characteristic facies in the Agardhfjellet Formation and occurs as sandy/silty carbonate beds, with scattered glauconite and phosphatic grains (Fig. 13). Carbonate minerals include dolomite, ankerite, siderite and rarely calcite. The thickness of F7 beds typically ranges from a few centimetres to a decimetre, but occasionally up to 1 m. Bivalves, gastropods and few ammonites and belemnites occur on the top surfaces of some of these beds, while other beds are packed with ammonites, bivalves, belemnites, scattered vertebrate bones, wood fragments and crinoids (e.g., the informal *Dorsoplanites*

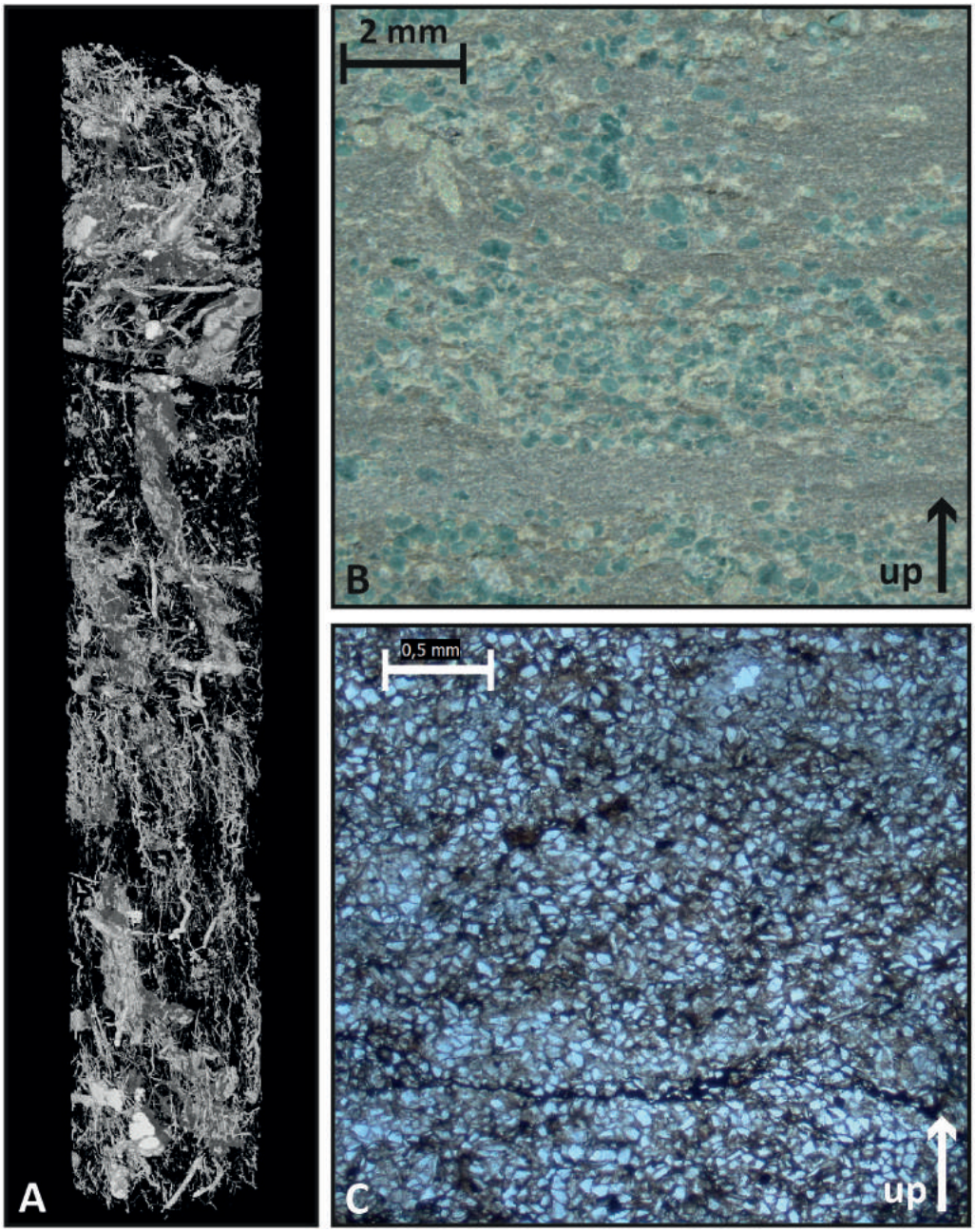

Figure 10. *(A) CT-image of the Myklegardfjellet Bed at 479.26–479.00 m in DH2 showing a completely burrowed part of the bed. (B) Microscope view of the glauconite grains of the Myklegardfjellet bed suspended in the matrix, accompanied by pyrite. Note very thin lamination. (C) Microscope image from 730 m in DH2. The core diameter is about 6 cm.*

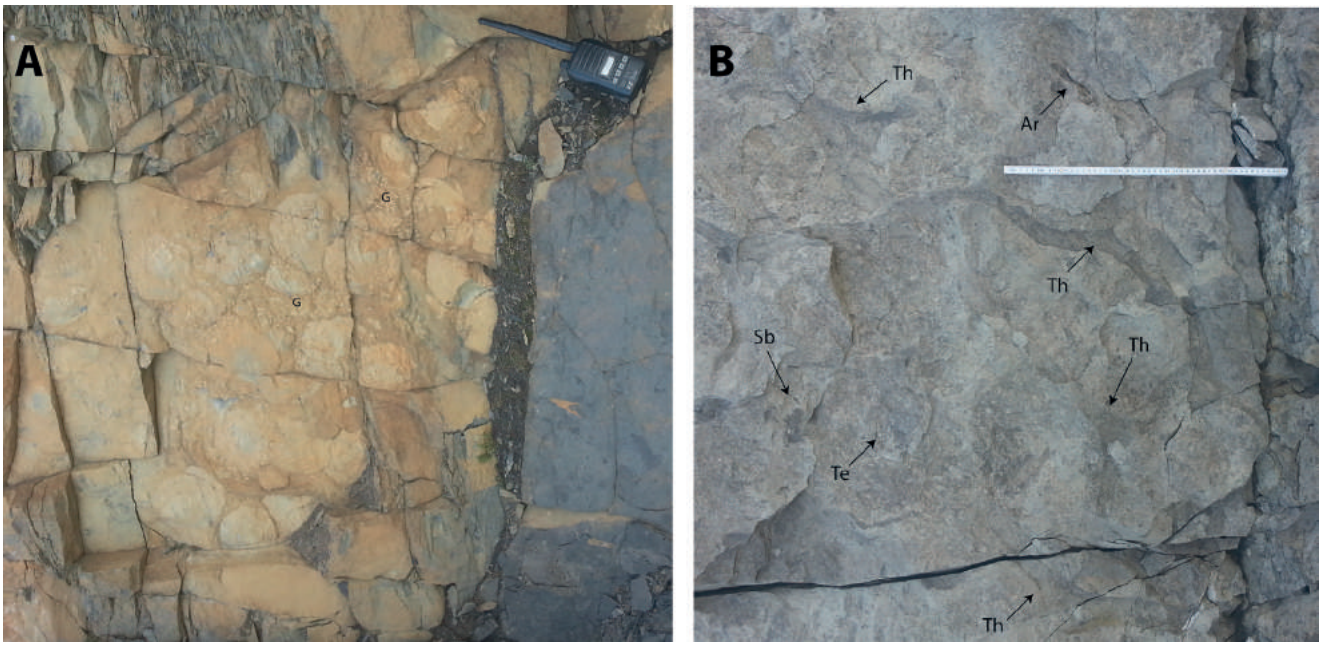

Figure 11. *(A) Top surface of a sandy carbonate bed, F7, with large bivalve shell fragments and gastropods 'G' interpreted as a condensed bed; FA 2 (cf., the* 'Pecten-*Bank' reported from the Kimmeridgian at Festningen by Sokolov & Bodylevsky, 1931). The VHF Radio is 10 cm wide. (B) Burrowed fine-grained sandstone, F4, from upper surface of a coarsening-upward unit; FA 3 to 4. Abbreviations: Ar* – Arenicolites, *Sb* – Schaubcylindrichnus, *Te* – Teichichnus. *Th* – Thallassinoides. *The stick is 50 cm. Both pictures are from the Oppdalssåta Member, Festningen, Isfjorden.*

bed) and might be classified as coquinas. The fine- to medium-grained glauconitic sandstone bed (F6) is up to 0.5 m thick and in the study area this facies occurs in the middle part of the formation in both of the wells and the nearby outcrops and acts as a correlative bed.

The upper boundary of the Agardhfjellet Formation is defined by the base of the Myklegardfjellet Bed (Mørk et al., 1999). A description of this bed is nonetheless included here as it is interpreted to belong to FA 2. The Myklegardfjellet Bed occurs in outcrops as a shale with large dark-green glauconite grains (Fig. 10). This bed is heavily bioturbated (Figs. 10A, C) and is completely devoid of macrofossils. The bioturbation masks any pre-existing sedimentary structures. In the field, the Myklegardfjellet Bed is a strong marker unit as it weathers into green unconsolidated plastic clay, resulting from the decomposition of glauconite (Dypvik et al., 1992).

FA 2 is easily recognised on wireline logs. Carbonate beds (F7) in FA 2 show low gamma readings but peaks on the velocity log. Sideritic beds show very high magnetic susceptibility readings. The cleaner glauconitic beds (F6) show the opposite response with high gamma values, low velocity values and high magnetic susceptibility.

Interpretation: The base of the Marhøgda Bed, i.e., top surface of the Brentskardhaugen Bed with stromatolites and agglutinated foraminifera (Krajewski et al., 2001), is a correlative surface throughout Svalbard (Mørk et al., 1999) representing a marine omission surface. Based on a petrographic and diagenetic study, Krajewski (1990) interpreted the Marhøgda Bed as a result of change in water circulation at a very low sedimentation rate. Phosphate nodules probably formed at the base during transgressive events (Krajewski, 1990).

The dolomite/ankerite and siderite show isotopic compositions indicating formation during deep burial (Krajewski, 2004). However, they most likely originated from dissolution of beds rich in aragonite and calcite fossils. Isotopic work on the carbonate concretions and beds in the Agardhfjellet Formation revealed they were formed by a combination of dissolution of biogenic carbonate and thermal decomposition of organic matter (Krajewski, 2004). Siderite concretions with well-preserved echinoderms (Rousseau & Nakrem, 2012) in the Slottsmøya Member at Janusfjellet are consistent with previous calcite concretions or beds diagenetically altered to siderite during burial. Generally, fossiliferous carbonate beds within a predominantly siliciclastic shale unit suggest condensation, as muds tend to 'shut off' or dilute the production of biogenic carbonate (Walker et al., 1983). A few examples of well-preserved fossils with no sign of broken shells capping the top surface of carbonate beds suggest omission surfaces and deposition below storm wave base. Also, well preserved ammonites and bivalves often with both shells intact in highly fossiliferous carbonate beds, e.g., the *Dorsoplanites* bed, suggest deposition below storm wave base. It is then concluded that these beds do not represent allochthonous carbonate beds as, for example, storm beds, but they are rather a response to condensation by termination of clay and silt deposition.

Two beds constitute the glauconitic facies (F6). Glauconite is generally seen as grains replacing minerals or small amorphous clusters in the formation. The glauconite beds suggest mostly an autochthonous or parautochthonnous origin. Glauconite is commonly formed in open-marine environments with very low sedimentation rates (Odin & Matter, 1981).

In the lower part, glauconite sandstone beds are overlying the top surface of the Brentskardhaugen Bed and are followed by a monomict phosphate conglomerate (Rismyhr et al., in press). Glauconite associated with phosphate is commonly interpreted as due to condensation, although reworking in active tectonic basins can produce allochthonous glauconite (Amorosi, 1997). The top surface of the first coarsening-upward unit in the Oppdalssåta Member (Figs. 2, 17) is also capped by dm-thick glauconitic sandstone in all wells and nearby outcrops at Janusfjellet and Konusdalen, and functions as a correlative surface in Adventdalen. F8 suggests that there was a temporary slowdown of clay and silt sedimentation on the sea floor.

To conclude, FA 2 represents deposition under very low accumulation rates, i.e., condensation. Lack of sedimentary structures and well preserved body fossils indicate protected deposition and sediment starvation. This, together with a variable marine invertebrate fauna including common ammonites, bivalves and belemnites, suggests an open marine shelf depositional environment. FA 2 was probably deposited below storm wave base, distal from the source area, or alternatively the lack of sediment may have resulted from large-scale delta shifts, avulsion. However, the origin of the Myklegardfjellet Bed is still enigmatic and it might represent a much shallower water depth.

FA 3: Transition zone/Prodelta

Description: FA 3 occurs as tabular bodies in the study area. This facies association consists mainly of heteroliths (F3), interbedded grey silty shale (F2) and burrowed very fine-grained sandstone (F4; Fig. 13). Normally, FA 3 occurs above FA 1 and in the middle part of coarsening-upward (CU) units overlain by FA 4. In the Slottsmøya Member, FA 3 never passes upward to FA 4 but is

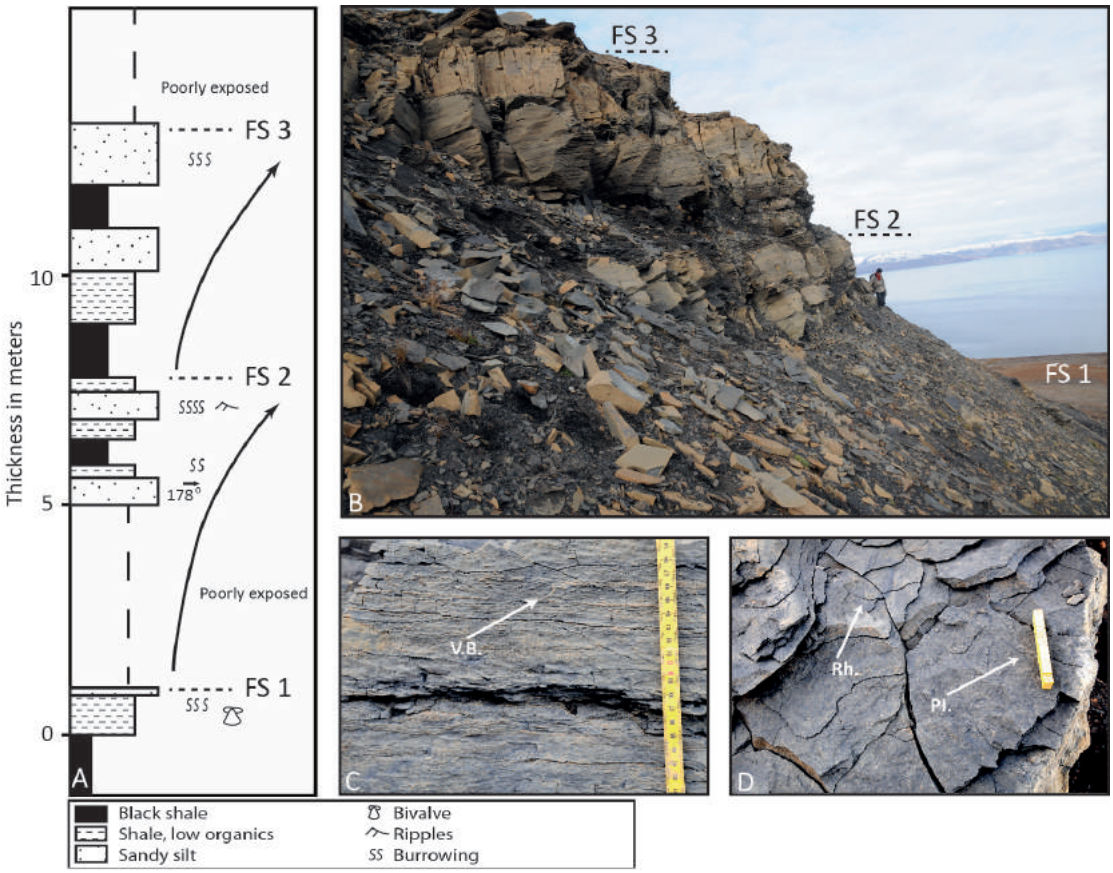

Figure 12. *Three CU units comprising FA 3 passing up to FA 4 and belonging in the Kimmeridgian (upper part of the Lardyfjellet Member and Oppdalssåta Member). (A) Logged succession: A flooding surface (FS 1) above a poorly exposed CU unit followed by two CU units. (B) The three CU units show gradually thicker sandstone beds upwards suggesting an overall prograding succession or regressive sequence. See Fig. 2 for comparison with borehole DH5R. (C) FA 3: Planar-parallel stratification and ripples intersect burrowed very fine-grained sandstone, from the middle part of second CU unit (V.B. = vertical burrow). (D) FA 4: Bedding surface from upper part of upper CU unit with Rhizocorallium (Rh.) and Planolites (Pl.) burrows. The section is from the valley between Criocerasaksla and Wimanfjellet.*

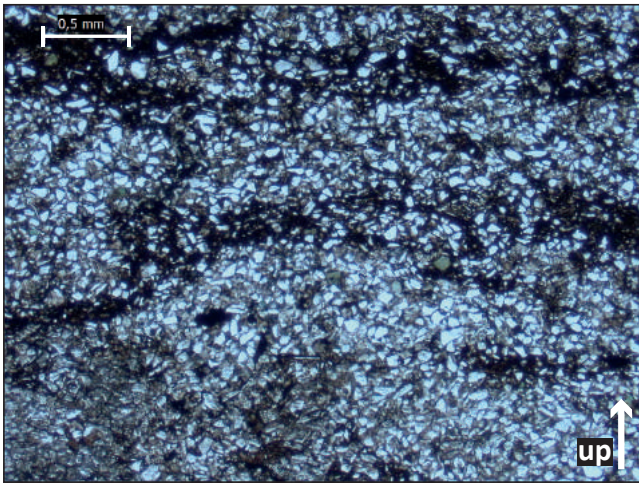

Figure 13. Thin-section of burrowed, very fine, muddy sandstone with scattered glauconite grains, F4 and FA 3. Near the top of the Oppdalssåta Member in DH2, 608 m.

normally overlain by offshore shale (FA 1) or condensed units (FA 2). In rare cases, hummocky cross-stratified sandstone (F4) has sharp boundaries towards an underlying black paper shale (F1; Fig. 14), then overlain by heteroliths (F3) of FA 3. In fining-upward (FU) units, FA 3 occurs in the lower or middle parts. Hummocky cross-stratified, laminated and current-rippled and very fine-grained sandstone beds (F4) in places intersect the main lithology in FA 3. In the uppermost part of the Slottsmøya Member, approximately 30 m below the base of the Rurikfjellet Formation (Myklegardfjellet Bed), a 20 m-thick diamictite unit with amalgamated beds of matrix-supported, poorly sorted mud clasts and quartz grains (F5), intersects the silty shale of FA 1 in DH5R, and is assigned to FA 3. The diamictite shows no fining- or coarsening-upward trend. The sandstone beds in FA 3 are commonly carbonate cemented, convolute-bedded and normal graded beds from siltstone to very fine-grained sandstone.

Siderite concretions are generally flattened discos-shaped bodies and can reach a considerable size with a diameter up to 4–5 m. *Chondrites, Planolites, Nereites* and rare occurrences of *Palaeophycus* trace fossils are observed, but bioturbation is generally relatively low within FA 3. Ammonites, belemnites, some bivalves and gastropods and rare wood fragments are also observed. Several marine reptiles are found in this facies association (Hurum et al., 2012; Delsett et al., 2016). The gamma log shows a cylinder to funnel shape with highly serrated traces. The base of the diamictite shows a sharp increase in velocity (Fig. 17).

Interpretation: Scattered hummocky cross-stratified beds (F4) in a heterolithic facies (F3) and the stratigraphic position between outer shelf or offshore shale (FA 1) and the coarser-grained lower shoreface or delta front (FA 4) both suggest transition zone deposits (cf., Howard & Reineck, 1981). Planar-parallel stratification (PPS; also reported by Dypvik et al. (1991b) in a location 20 km southeast of Janusfjellet) and current ripples suggest additional traction-generated structures, indicating distal hyperpycnal flow deposits (Mulder et al., 2003). The shales might represent a combination of muddy turbidites from river-fed hyperpycnal flows and mud settled from hypopycnal plumes (Parsons et al., 2001). Later bioturbation destroyed the originally laminated deposits. Deformation of sediments in prodelta deposits is commonly caused by prograding deltas (Galloway & Hobday, 2012). The diamictite (F5), interpreted as a debris flow, is then suggested to be a result of slope failure in a prodelta setting. The sudden increase in velocity is consistent with a more homogeneous mud-supported debris flow, suggesting more compacted high-density sediments during deposition (Mulder & Alexander, 2001).

FA 3 is generally found in the lower-middle part of a CU unit (Fig. 12) which suggests it is part of a prograding shoreline or delta.

FA 4: Shoreface/Delta front

Description: This facies association is well recognised on wireline logs as showing low gamma and high velocity as a result of the high degree of cementation of the sandstone (Fig. 4). The sandstones correspond to peaks in Zr/Rb ratios, with values from c. 8 to more than 15 (Fig. 6). It is normally either capping a coarsening-upward (CU) unit or is part of one. This FA consists of intensely burrowed, grey-coloured, very fine to fine-grained sandstones, often intersected by up to 30–60 cm-thick hummocky cross-stratified beds. In places. the hummocky cross-stratified beds have a lag of broken gastropod and bivalve fragments.

The sandstones in FA 4 are quite commonly dolomite cemented and weather to a yellowish colour in outcrops. FA 4 has the most diverse trace fossil assemblage in the Agardhfjellet Formation. *Skolithos*, *Palaeophycus,* small *Chondrites* and *Teichichnus* are common throughout FA 4, while *Arenicolites and Rhizocorallium* occur mostly in the upper part of the CU units suggesting a mixture of *Skolithos* and *Cruziana* ichnofacies (Fig. 11).

Gastropods are common in some beds, mainly in the Oppdalssåta Member. A very fine to fine-grained, 1.5 m-thick burrowed sandstone of the Oppdalssåta Member in the Festningen section shows a rich and diverse trace-fossil assemblage. The following trace fossils are identified: *Phycosiphon incertum*, *Teichichnus rectus, Schaubcylindrichnus coronus*, *Siphonichnus ophthalmoides*, *Skolithos* isp., *Taenidium* isp., *Thalassinoides* isp. and *Rosselia* isp. (Dirk Knaust, pers. comm., August 2017).

FA 4 is normally overlying prodelta facies (FA 3) or offshore shale (FA 1) and in places is capped by the

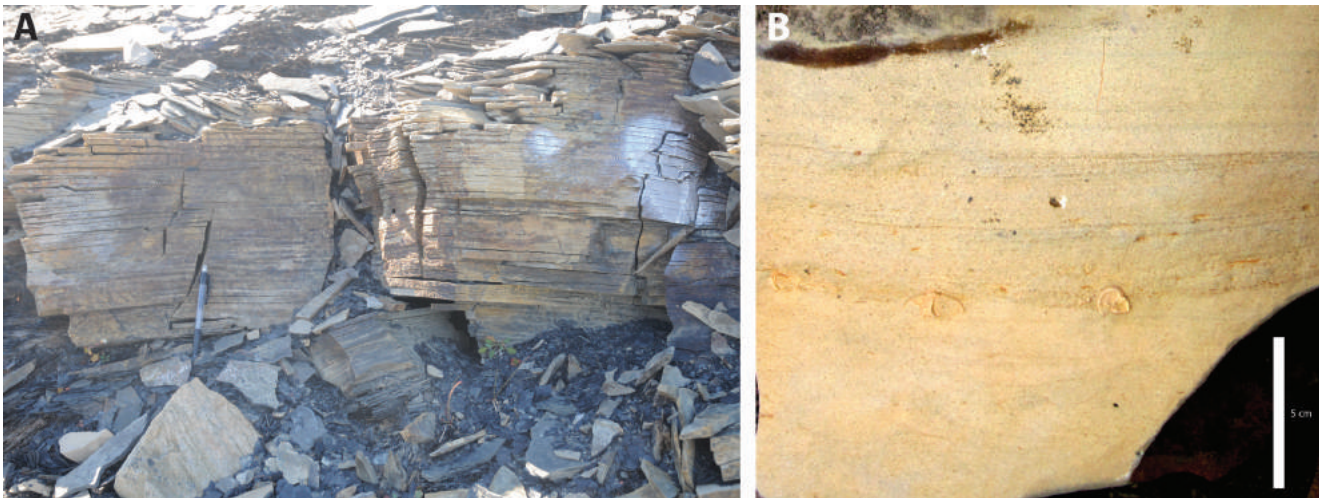

Figure 14. *(A) Rare, thick, single-storey hummocky cross-stratified sandstone bed F4 in FA 4. Note the convex up laminae and low-angle truncation of laminae (stippled), Oppdalssåta Member at Janusfjellet. (B) Very fine-grained carbonate-cemented sandstone bed from the Oppdalssåta Member, Janusfjellet. The lower part is homogeneous and the lack of structures is probably caused by bioturbation. The upper half starts with a subtle erosive surface overlain by a lag of broken fossil fragments with gastropods, which fines upward (less coarse fossil fragments) to laminated very fine-grained sandstone. This upper half is interpreted as a tempestite in FA 3.*

condensed facies of FA 2. In a locality in northeast Adventdalen, a 4–5 m-thick, well-organised CU unit is resting on black paper shale of FA 1 in the upper part of the Oppdalssåta Member (Fig. 15). This CU unit is organised as interbedded very fine-grained sandstone and burrowed siltstone and with heteroliths of FA 3 at the base. This basal part is passing upward to two amalgamated hummocky and swaley cross-bedded, very fine-grained 1.0 and 1.5 m-thick sandstone beds (FA 4) separated by a 20 cm-thick shale bed. The upper amalgamated bed is followed by a 30 to 40 cm, fine-grained, glauconitic dolomite-cemented sandstone bed with faint trough cross-stratification (Fig. 15). The CU unit is capped by a laterally consistent belemnite, ammonite and bivalve-rich condensed sandy carbonate bed with numerous wood fragments and logs assigned to FA 2. This CU unit gradually thins laterally and pinches out towards the northeast to burrowed, grey-coloured, very fine-grained bedded sandstone with a few hummocky cross-stratified beds (Fig. 15). The CU unit is overlain by organic-rich shale FA 1 with a few wood fragments, logs and common bivalves. The gamma and velocity logs have a typical serrated funnel shape for the CU units (Fig. 4) and a serrated bell shape for the FU unit.

Interpretation: FA 4 is seen as the uppermost FA in the well-organised CU units (Figs. 12 & 15) particularly in the Lardyfjellet Member and Oppdalssåta Member. FA 4 and the CU units from siltstone to fine-grained sandstone (Fig. 14) in the Oppdalssåta Member were interpreted by Dypvik et al. (1991b) as shelf sand ridges, later termed offshore sand bars (Dypvik et al., 2002). Due to full core coverage combined with wireline logs, detailed studies of nearby outcrops (i.e., northeast Adventdalen), improved biostratigraphy, palaeontology and a diverse recognised trace-fossil assemblage, it is possible to give an alternative interpretation.

The majority of sedimentary structures in FA 4 are generated by mixed oscillation and traction currents. The scattered hummocky cross-stratified sandstone beds in the more heterolithic FA 3 become amalgamated upward to FA 4, with hummocky and swaley cross-bedding, which then represents a shallowing-upward deposition, probably from a prograding wave-dominated shoreline (cf., Walker & James, 1992; Dumas & Arnott, 2006). The rich ichnofauna indicates general shallow-marine conditions in a well-oxygenated environment, probably in a lower shoreface setting or distal delta front (Frey et al., 1990, Knaust & Bromley, 2012; Knaust, 2017). Layers with a mass occurrence of *Siphonichnus ophthalmoides* were interpreted by Knaust (2015) as caused by fluctuating salinity linked to freshwater influx due to the close vicinity to a deltaic environment (Knaust, 2015). The majority of CU units in the Oppdalen Member in our study area are suggested to shallow up to the lower shoreface or lower delta front. The well-defined 4–5 m-thick CU unit with thicker amalgamated hummocky and swaley cross-stratified beds in northeast Adventdalen pinches out only tens of metres laterally (Fig. 15) and is interpreted as a remnant of a wave-dominated delta front (Pratt et al., 1992). The low-angle trough cross-stratified very fine-grained sandstones in the upper part represent middle shoreface or more proximal delta-front deposits. The isolated bodies are probably a result of a delta-lobe shift in a wave-agitated basin. The overlying, laterally consistent, condensed facies (FA 2) is possibly due to a sudden relative sea level rise or delta-lobe abandonment. Both processes will terminate sediment input to the basin, i.e., producing a starved basin.

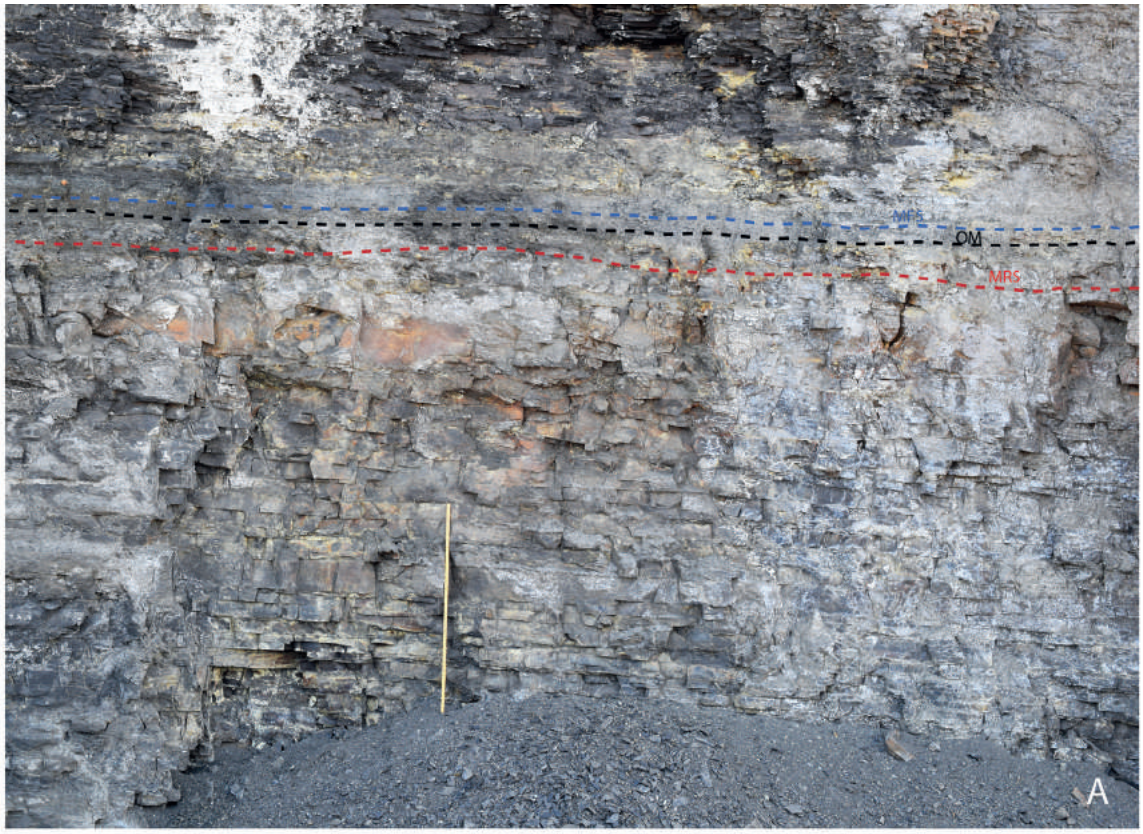
MFS
OM
MRS
A

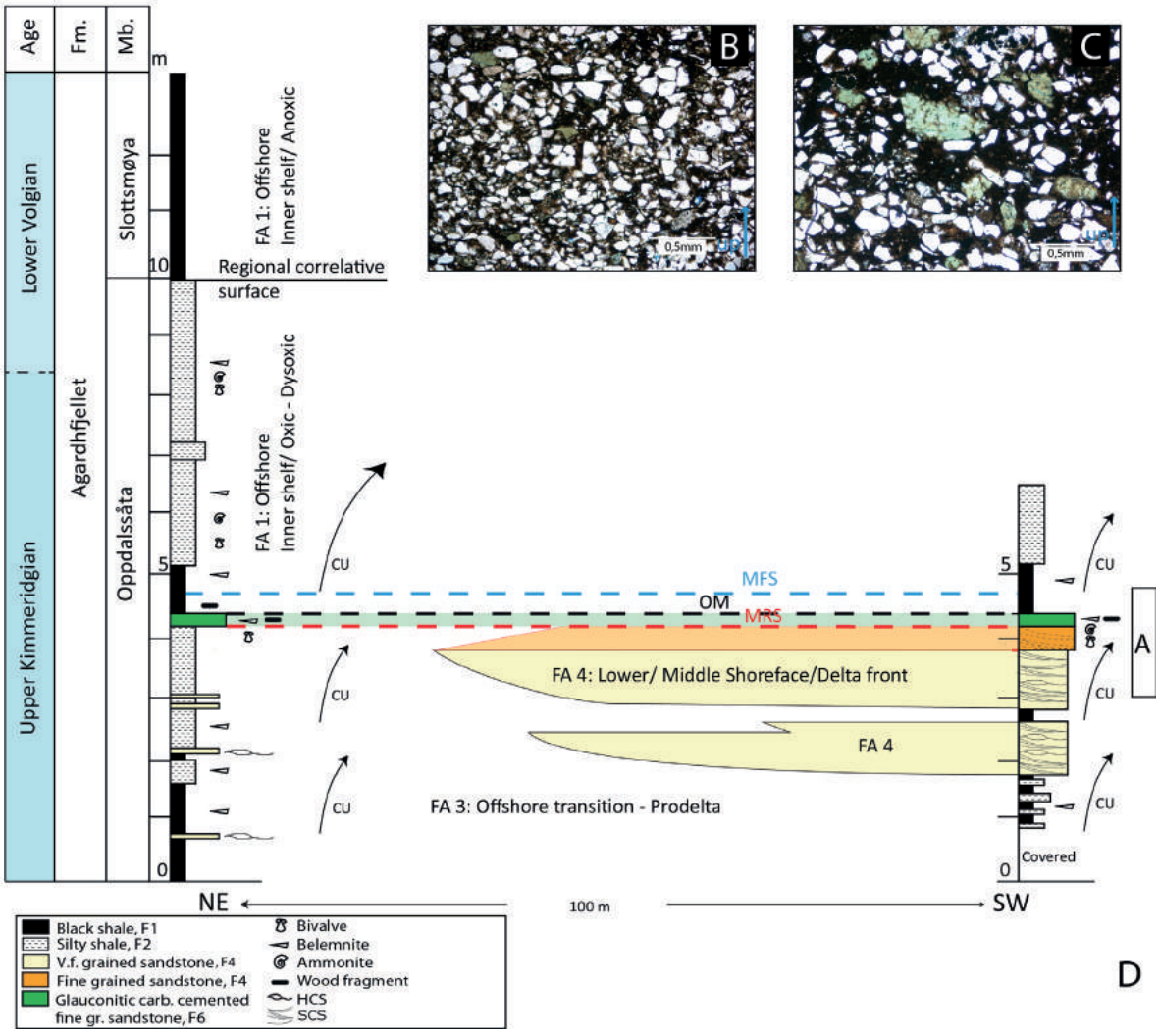
Age
Fm.
Mb.
Lower Volgian
Upper Kimmeridgian
Agardhfjellet
Slottsmøya
Oppdalssåta
m
10
5
0
Regional correlative surface
FA 1: Offshore Inner shelf/ Anoxic
FA 1: Offshore Inner shelf/ Oxic - Dysoxic
B
C
0.5mm
CU
MFS
OM
MRS
A
FA 4: Lower/ Middle Shoreface/Delta front
FA 4
FA 3: Offshore transition - Prodelta
Covered
NE
100 m
SW
Black shale, F1
Silty shale, F2
V.f. grained sandstone, F4
Fine grained sandstone, F4
Glauconitic carb. cemented fine gr. sandstone, F6
Bivalve
Belemnite
Ammonite
Wood fragment
HCS
SCS
D

Towards a sequence-stratigraphic model of the Bathonian to Ryazanian succession in central Spitsbergen

Stacking pattern of the facies associations

As shown above, we have subdivided the Agardhfjellet Formation into four facies associations (Table 2). The facies associations are coupled mainly to CU and rare FU units. The CU units are normally organised in an ascending order from offshore (FA 1), via transition zone/prodelta (FA 3), to lower middle shoreface/delta front (FA 4). These stacking patterns of CU units are interpreted as distal responses to prograding coastlines/deltas. The condensed FA 2 is more problematic and might represent both offshore and inner shelf depositional environments. In the latter case it caps or constitutes the upper part of the CU units. Glauconite beds or glauconitic sandstones (Fig. 10B) are mostly associated with the transgressive systems tract and maximum flooding surfaces (Loutit et al., 1988; Amorosi, 1995; Amorosi et al., 2012). The lower part of the formation, the Oppdalen Member, is organised as a well-defined FU unit and commonly with a condensed unit, FA 2, in the lower part (the Marhøgda Bed) containing glauconite (F6), monomict phosphate and a carbonate bed (F7). This is followed by FA 3 and capped by FA 1, indicative of a transgression or back-stepping of a coastline.

Agardhfjellet Formation organised as clinoforms

Clinoform geometries are not observed in outcrops or in seismic data in this study. However, geometries can also be deduced from the stacking pattern of facies (Helland-Hansen & Hampson, 2009). The numerous well organised CU units and their facies associations in the Agardhfjellet Formation suggest that the formation is attributable to foreset and bottomset depositional profiles as defined by Steel & Olsen (2002). The thicknesses of the deduced clinoform units suggest that they represent shoreline clinoforms at a scale of metres to tens of metres in height, as defined by Helland-Hansen & Hampson (2009). The shoreline clinoforms are produced by prograding deltas, strandplains and barrier islands. From core descriptions and wireline log motifs the two middle members, Lardyfjellet Member and Oppdalssåta Member, form well defined CU units (Fig. 17). These CU units comprise from base: offshore (FA 1) via transition zone/prodelta (FA 3) to distal delta-front/lower middle shoreface facies associations (FA 4). The CU units are commonly capped by condensed facies associations (FA 2). These stacking patterns of the facies associations are interpreted to represent clinoforms with bottomsets, slope and foresets, respectively.

FA 3 and 4 show beds with hummocky cross-stratification indicative of having been deposited within the storm wave base (Dumas & Arnott, 2006). Sedimentary structures or ichnofacies are not necessarily indicators of water depth as penetration of waves to sea floor varies from larger to smaller oceans. For example, from the Gulf of Mexico to the Atlantic side of Florida, wave base changes from 50 m to 100 m (Peters & Loss, 2012). Fair-weather wave base typically occurs at a depth from 5 to 20 m (Nichols, 2009). The CU units in Konusdalen (Fig. 12) with *Cruziana* ichnofacies are indicative of low-energy marine depositional environments near storm wave base (Frey et al., 1990). Although neither decompaction nor basin subsidence is taken into consideration, the stacking pattern of the CU units, i.e., the clinoforms, gives some indication of water depths during deposition of the Agardhfjellet Formation. A nearly 40 m-thick CU unit is seen from 627 m to 575 m in borehole DH5R, in the Lardyfjellet Member and Oppdalssåta Member (Fig. 17). This is the thickest continuous CU unit in our study area and suggests water depths of tens of metres during progradation. This is a scale comparable to subaqueous clinoforms as described by Helland-Hansen & Hampson (2009). These observations, taken together, indicate a storm wave base of less than 50 m in this basin. The more subtle CU units in the Slottsmøya Member, which only reach the lower slope facies association (FA 3) as the most proximal facies, are also suggested to have been deposited in relatively shallow water (Nagy et al., 1990; Hammer et al., 2011; Collignon & Hammer, 2012; Hryniewicz et al., 2012). Furthermore, the biota, particularly foraminifers, suggest that this member also was deposited in shallow water within an epicontinental sea (Nagy et al., 1990; Dypvik et al., 1991b; Nagy & Basov, 1998). Here, the clinforms represent a more distal depositional environment than the Lardyfjellet Member and Oppdalssåta Member.

As the top set, i.e., foreshore or coastal/delta plain deposits, is not observed in the CU units in the Agardhfjellet Formation, the majority of CU units in the formation are probably deposited as subaqueous clinoforms. One exception is the sandstone body in Adventdalen (Fig. 15) which is interpreted as a delta-

Figure 15. *Outcropping sandstone unit in the Oppdalssåta Member, northeast Adventdalen. (A) FA 4 with amalgamated hummocky (HCS) and swaley (SCS) cross-stratified very fine-grained sandstone in lower 1.5 m part passing upward to faint trough cross-stratified fine-grained sandstone, probably migrating dunes, F4. Above the black stippled line; black paper shale, F1, is sharply overlying the sandstones, The red line marks the onset of carbonate-cemented sandstone and represents the MRS. The MFS is marked by the blue stippled line. The stick is 1 m and the picture is marked with a bar in (D). (B) Thin-section showing very fine-grained moderately sorted sandstone with glauconite grains of the middle part of the sandstone succession, coloured yellow in (D). (C) Poorly sorted dolomite-cemented glauconitic fine-grained sandstone from the upper part of the sandstone unit, coloured orange to green in (D). (D) Logged succession of the outcrop. The more homogeneous sandstone unit is pinching out to the SW, with a more heterolithic and silty succession in the NE.*

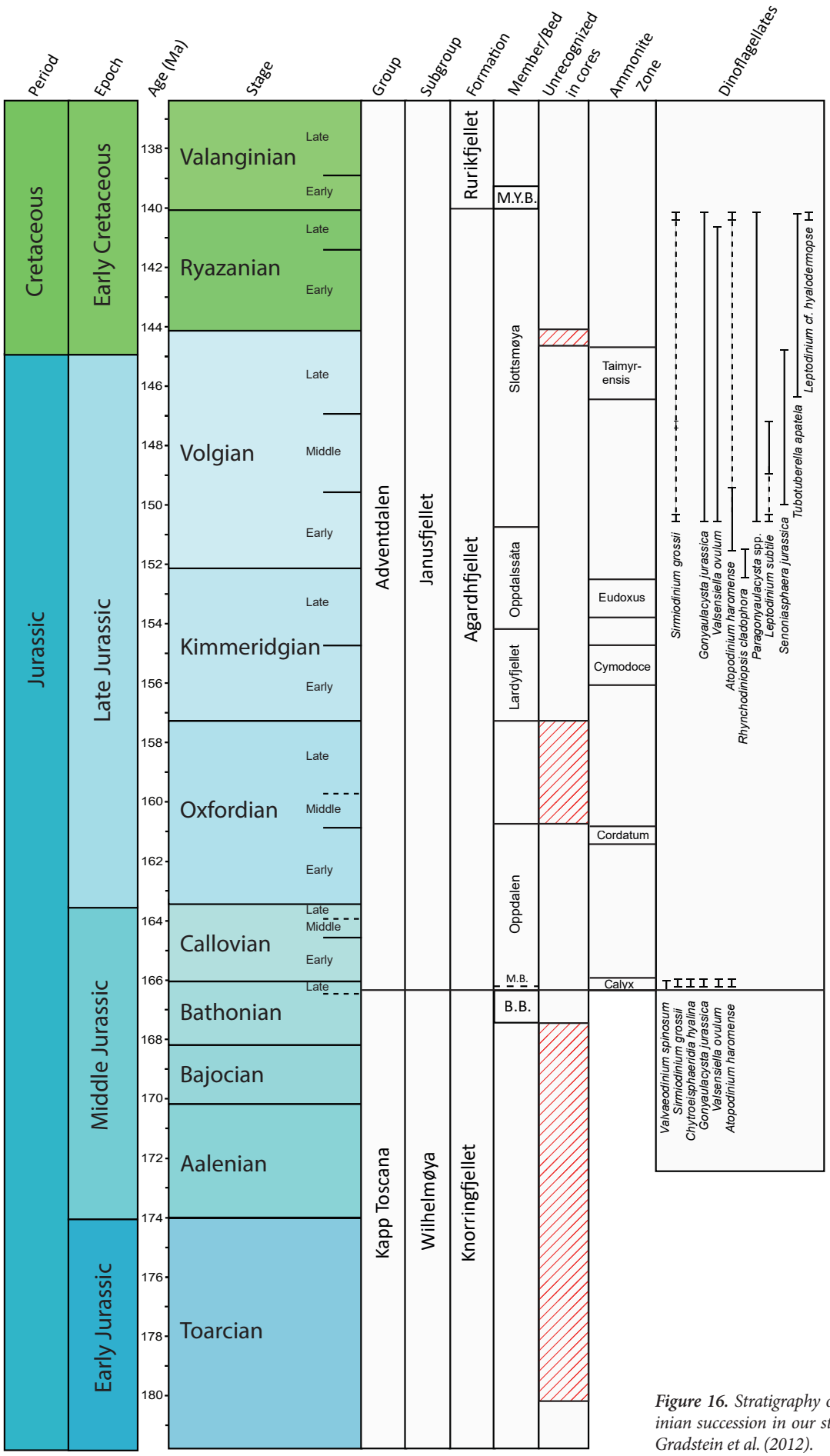

Figure 16. *Stratigraphy of the Toarcian to Valanginian succession in our study area. Time scale after Gradstein et al. (2012).*

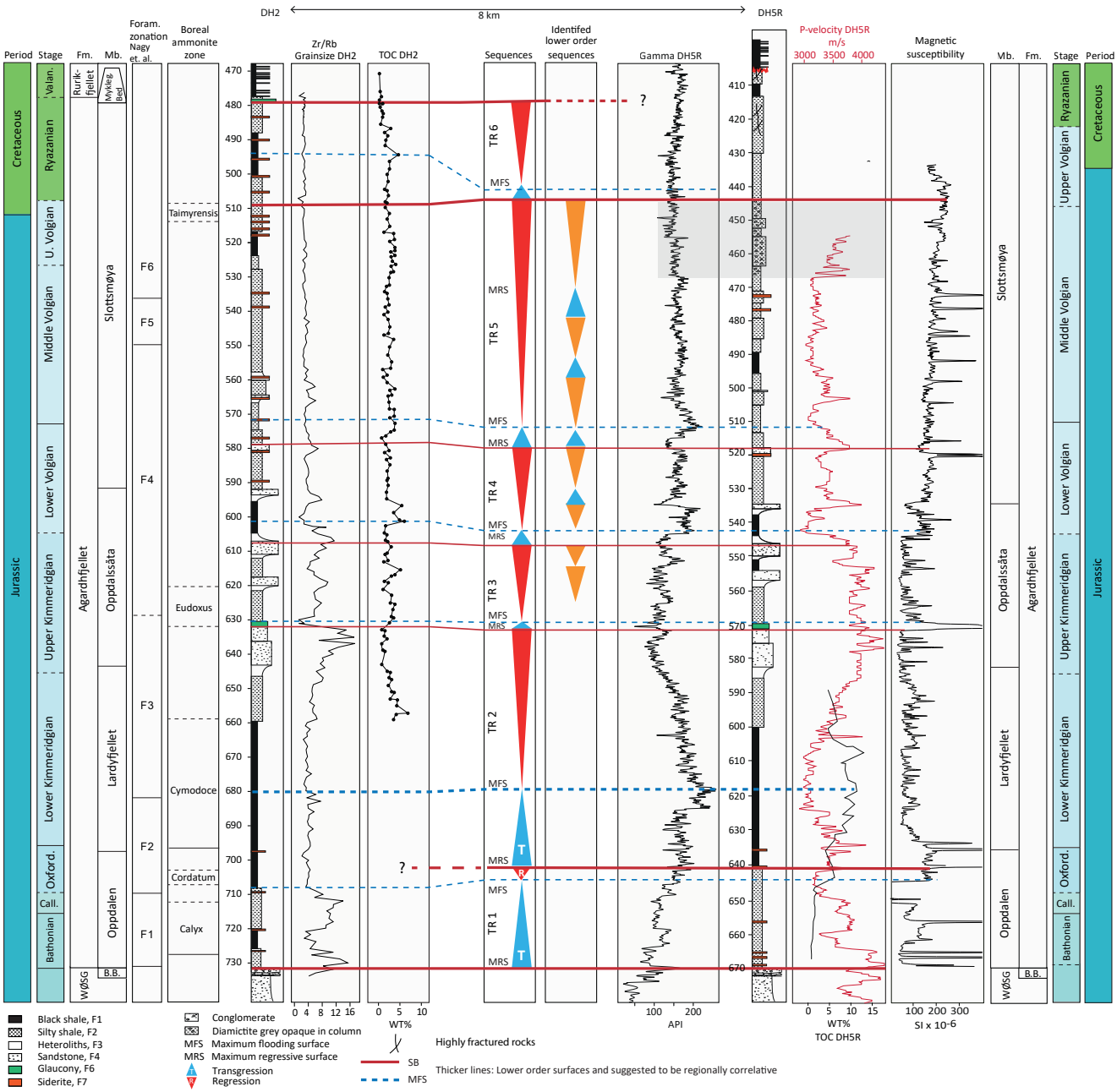

Figure 17. *Suggested sequence stratigraphy of the Agardhfjellet Formation based on wells from Adventdalen. The stippled blue line and the red line are drawn to the log motifs which give the best definition of the MFS and MRS, respectively. As the upper part is close to a major thrust fault, i.e., the upper decollement zone in the study area, there is some concern of the validity of TR 6 in DH5R. Also, the debris deposits (the diamictite bed, marked in grey in the figure) give some uncertainty to TR 6 in DH5R.*

front deposit with an almost preserved top set (middle shoreface). This CU unit might be classified as a shoreline clinoform or even originally as a part of a subaerial delta clinoform event (cf., Helland-Hansen & Hampson, 2009). The missing, expected, top-set deposits might have been truncated or most likely distally deposited and reworked during a transgressive event (cf., Helland-Hansen & Hampson, 2009).

Sequence-stratigraphic subdivision

In our study area, the Agardhfjellet Formation is bounded by two key sequence-stratigraphic surfaces which also define the lithostratigraphic boundaries of the formation (Mørk et al., 1999). The lower lithostratigraphic boundary is the top of the Brentskardhaugen Bed. This top surface is interpreted as an omission surface (Rismyhr et al., in press) and if present is also the base of the Bathonian Marhøgda Bed. The upper boundary surface of the Agardhfjellet Formation is also the base of a condensed bed; i.e., the Myklegardfjellet Bed of

probably latest Ryazanian–earliest Valanginian age. As discussed by Wierzbowski et al. (2011), the Early Ryazanian ammonite *Borealites* reported from the Myklegardfjellet Bed by Basov et al. (1997) may rather have come from the topmost Agardhfjellet Formation, based on lithology. Due to the unsolved facies interpretation of the Myklegardfjellet Bed (see discussion above) the nature of the upper sequence-stratigraphic surface is problematic, but it roughly coincides with the familiar so-called Base Cretaceous Unconformity (BCU) in the Barents Sea (Faleide et al., 1993, 2008; Smelror et al., 2001). These two key sequence-stratigraphic surfaces are also correlative into the Barents Sea. The top surface of the Realgrunnen Subgroup is correlative with the lower surface, while the upper surface, BCU or base Myklegardfjellet Bed, is correlative with the base of the Klippfisk and Knurr formations (Smelror et al., 1998; Worsley, 2008; Henriksen et al., 2011). These surfaces are not necessarily regionally chronostratigraphic.

By combining the stacking pattern of facies from cores and outcrops, wireline logs, TOC, magnetic susceptibility and Zr/Rb values with the biostratigraphy, we have defined six transgressive and regressive (TR) sequences, TR 1 to TR 6 (Fig. 16 & 17), which we believe might provide a framework for regional correlative surfaces. In addition, there may be Bajocian, Oxfordian and Valanginian hiatuses or at least condensed intervals, i.e., sequence boundaries, in the cores described here. This is indicated by possibly missing Bajocian strata (Bäckström & Nagy, 1985), the lack of recognised Middle/Upper Oxfordian strata (Fig. 16) and the near base Valanginian unconformity surface (BCU). Also, the transition between the Volgian and Ryazanian is poorly represented (cf., Wierzbowski et al., 2011). We have subdivided the Bathonian to latest Ryazanian into six informal TR sequences. We recognise that the lower and upper boundary surfaces of the the Agardhfjellet Formation (i.e., the Bajocian hiatus and the near Valanginian base, BCU, respectively), the near top Oppdalen Member, i.e., top of TR 1, and near the boundary between the Volgian and Ryazanian, i.e., top of TR 5, are of more correlative importance regionally (Fig. 17). While TR 1, 2, 3 and 4 are well defined, the fine-grained nature of TR 5 and 6 make interpretation of prograding and retrograding trends more challenging. In TR 3, 4, 5 and 6 (Fig. 17), potential higher-order sequences have also been identified.

Embry (1993) and Embry & Johannessen (1993) used the combination of subaerial unconformity (SU), shoreline ravinement surface (SR–U) and maximum regressive surface (MRS) as basin-wide sequence-stratigraphic boundaries. In wells, the maximum regressive surface occurs near either the top coarsest siliciclastic unit or the lowest gamma and highest velocity readings of a CU unit. In outcrops, the MRS are picked near or just below the top surface of the proximal facies within a prograding CU unit. It is commonly seen as the base of a carbonate-cemented sandstone or a surface with a sudden increase in bioturbation. The reasoning for picking the MRS at these levels is that it indicates less energy or drowning and thereby the turning point from prograding to retrograding. However, due to either an unclear age or disputed dating, the basal boundary surface is picked on the top surface, i.e., the omission surface of the Brentskardhaugen Bed in this study.

The bases of correlative condensed beds may also suggest sequence boundaries (Galloway, 1989). Glauconite beds and the most prominent carbonate beds seen as stratiform beds in outcrops suggest several levels of sediment starvation. Glauconite and siderite are expressed by a high magnetic susceptibility reflecting the presence of iron minerals whereas siderite or other carbonates give high velocity peaks. We have then chosen the most prominent condensed beds as MRS at the base and MFS on the top surface of these beds. This means that we separate MRS from MFS as the bed might include a longer time span. A sudden change to a more silt content in the shales or vice versa might also be indicative of sequence-stratigraphic surfaces based on the assumption of a change from a distal to a more proximal facies (Macquaker & Gawthorpe, 1993). An increase in TOC values is most likely a combination of higher organic productivity and less influx of clay and silt, and is probably due to raised relative sea level; thus, a candidate for picking the MFS. Below and in ascending stratigraphic order we describe the six TR sequences which span nearly 25 myr. Apart from TR 6, the available gamma and velocity logs and magnetic susceptibility from DH5R are used for the definition of TR sequences, but correlation towards the 7 km westward-distant DH2 based on sedimentological log, TOC and Zr/Rb curves seems well constrained. The layer cake correlation over this relatively short distance probably reflects the mostly distal deposits on a flat sea floor or perpendicular to the depositional dip within an area of gentle slope in a shallow epicontinental or sag basin.

TR 1

The SB of TR 1 is defined at the top of the Brentskardhaugen Bed. In addition to the Marhøgda Bed when present, it includes most of the Oppdalen Member . It varies in thickness from 27 m in DH2 to 30 m in DH5R. Apart from the Marhøgda Bed, the lower part of TR 1 is poorly exposed in most outcrops in Central wSpitsbergen.

Age: Bathonian to Oxfordian, with the *Calyx* and *Cordatum* zones.

Sedimentological expression: The Brentskardhaugen Bed is conformably overlain by, if present, a glauconitic chamositic carbonate with phosphatic ooids, and carbonate-cemented sandstone, FA 2, which is referred to as the Marhøgda Bed (Bäckström & Nagy, 1985). However, generally above the top surface, i.e., the omission surface at the top surface of the

Brentskardhaugen Bed, in cores TR 1 shows a subtle fining-upward (FU) trend from sandy to silty shale to shale with less silt content; F2. The FU trend is easier to recognise on the gamma log.

Sequence stratigraphic expression of the surfaces: The surfaces are based upon the wireline logs and the cores of borehole DH5R. The MRS of TR 1 is based on an abrupt change in velocity and higher gamma reading at 643 m. It is also recognised in the DH5R core by the transition from grey silty shale (F2) to black shale with a sudden increase in TOC (F1; Figs. 5 & 17). A gamma peak at 648 m and increase in TOC in borehole DH5R is suggested as the MFS in TR 1. The surfaces are not clear in borehole DH2, but we have used the top of the *Cordatum* zone as a possible hiatus in central Spitsbergen and thereby a potential sequence boundary within the Oxfordian strata in central Spitsbergen.

The transgressive nature of the lower part of the Oppdalen Member is well documented in Svalbard (Dypvik et al., 1991b; Nagy & Basov, 1998; Nagy et al., 2009).

TR 2

The SB of TR 2 is defined as the MRS of TR 1. It includes the uppermost part of the Oppdalen, the Lardyfjellet and the lower part of the Oppdalssåta members, and varies in thickness between 71 m in borehole DH5R and 73 m in borehole DH2. The SB of TR 2 is suggested to correlate to near the boundary surface between the Fuglen and the Hekkingen formations in the Barents Sea (cf., Smelror et al., 2001; Worsley, 2008).

Age: Oxfordian to Late Kimmeridgian. There may be a small hiatus between TR 1 and TR 2.

Sedimentological expression: Above the SB, a 21 m-thick black shale, F1, shows a gradual upward decrease in velocity and increasing TOC in borehole DH5R, suggesting a gradually more distal facies. A 40 m-thick well-defined CU unit follows which is a characteristic trend of TR 2 in both wells and outcrops. This CU represents the thickest prograding unit in the Agardhfjellet Formation. In core and outcrop the CU trend passes from black shale (F1) to silty shales (F2) and sandstones and from FA 1 to 3 and 4 in ascending order. Besides a gradual upward-coarsening grain size, it is characterised by log motifs showing high gamma and low velocity readings together with high TOC values in the lower part passing upward to gradually lower gamma and higher velocity readings and TOC values.

Sequence-stratigraphic expression of the surfaces: Black shale F1 rests on grey shale F2 above the sequence boundary; the MRS of TR 1. There is an abrupt upwards change in the gamma log motifs from blocky to serrated while velocity increases and then gradually decreases in DH5R. We suggest that this is related to the carbonate content in the shale. At 623 m in borehole DH5R, both gamma and velocity logs show a shift in log motifs with higher gamma and lower velocity readings, and increased TOC. The MFS of TR 2 is defined as the highest gamma reading at 617 m in borehole DH5R, while the remaining 40 m-thick CU unit is the regressive system tract. A consistent, up to 1 m-thick, glauconite bed at 630 m in borehole DH2, 570 m in DH5R, and also seen at Janusfjellet (Fig. 2) represents a longer period of sediment starvation. It gives a high magnetic susceptibility peak in both borehole DH2 and DH5R, reflecting the iron content of the glauconite. Condensed beds normally occur in the transition between regressive and transgressive deposits (Galloway, 1989). The MRS of TR 2 is then placed at the base of this condensed bed.

TR 3

The SB is defined as the base of a nearly 1 m-thick, correlative glauconite bed in wells and nearby outcrops (Figs. 2 & 17). TR 3 is conformably overlying TR 2. The sequence is 34 and 35 m thick in boreholes DH2 and DH5R, respectively. This TR sequence occurs in the middle part of the Oppdalssåta Member, and in cored successions the gamma-ray log motif reveals two CU units above the glauconite bed (Fig. 17). These CU units are probably comparable to the 15 m-thick succession with two CU units seen in outcrops in the valley between Criocerasaksla and Wimanfjellet (Fig. 12).

Age: Late Kimmeridgian.

Sedimentological expression: The consistent correlative greenish-coloured bed is seen in outcrops and glauconitic sandstone is observed at the same stratigraphic level in the cored section. The two CU units are here suggested as higher-order sequences in TR 3 (Fig. 17). An ammonite in the CU unit in the outcrop east of Adventdalen (Fig. 17), probably *Hoplocardioceras elegans*, suggests the same age as TR 3 and it probably represents the upper CU unit in the boreholes. This outcrop, as well as other outcrops (Fig. 17) in central Spitsbergen, show similar CU units which pass from black paper shale to sandstones; FA 1, 3 and 4, with either abrupt or gradual transition from sandstones to paper shale above.

Sequence-stratigraphic expression of the surfaces: Both the SB and MFS are defined by the glauconite bed. While the SB of TR 3 is placed at the base of the glauconite bed, the MFS is on the top surface of the same bed. The MRS of TR 3 is well defined in the Adventdalen outcrop. Below the top surface of the CU unit, a 20–40 cm-thick, carbonate-cemented, burrowed upper part indicates a slowdown of sedimentation; a turnover point which is typical for an MRS (Embry, 1995). Although not clearly observed in the cored succession (although a strong Ca peak indicating carbonate cementation is seen in the XRF data at 603.5 m in borehole DH2), the same MRS is placed slightly below the top surface of the sandstone.

TR 4

The SB of TR 4 is defined as the MRS of TR 3 and is conformably overlying TR 3. The sequence occurs in the upper part of the Oppdalssåta Member and lower part of the Slottsmøya Member. It varies in thickness from 26 m to 29 m in outcrops at Janusfjellet and Deltaneset, and is 29 m thick in borehole DH5R and 28 m thick in borehole DH2. Above the MFS at c. 601 m in borehole DH2 and 542 m in borehole DH5R, TR 4 consists of two CU units which represent two higher-order sequences.

Age: Early Volgian.

Sedimentological expression: The lower transgressive part fines upward from thin silty shale bed F2 to paper shale F1.

Sequence-stratigraphic expression of the surfaces: As in TR 3, the MRS is placed at the base of a condensed unit. In this case it consists of a siderite bed on top of a CU unit. On log data, the MFS is located by the high gamma peak of a thin FU unit in borehole DH5R and coincides with a sudden increase in TOC and a low in the Zr/Rb curve in borehole DH2, indicating the finest grained sediments there. In the Janusfjellet and Konusdalen outcrops, details in this part of the Agardhfjellet Formation are obscured by weathering.

TR 5

The MRS of TR 4 is defined as the SB of TR 5 and is conformably overlying TR 4. In the boreholes DH2 and DH5R, TR 5 is 70 m and 74 m thick, respectively, and it occurs in the lower to middle part of the Slottsmøya Member. TR 5, as also TR 6, is weakly expressed, visible mainly only on gamma and velocity logs, and has not yet been recognised in outcrops. However, above the MFS in TR 5 two well defined CU units are recognised from cores and velocity and gamma log motifs, which represent two higher-order sequences.

Age: Early to Middle Volgian.

Sedimentological expression: The lower transgressive part fines upward from a thin bed of very fine-grained sandstone F4 to silty shale F2 to paper shale F1. The regressive part shows a mixture of facies associations; FA 1, 2 and 3.

Sequence-stratigraphic expression of the surfaces: As for sequence TR 3, the base of a condensed unit is defined as the MRS. The MFS is placed at the high gamma peak in borehole DH5R, which in cores is recognised in the lower part of a black paper shale unit. Thin, subtle, CU units are common in the Slottsmøya Member and although faintly expressed, some of them can be detected on the gamma and velocity logs (Fig. 17). They represent higher-order sequences which are included in the regressive part of TR 5.

TR 6

The SB of TR 6 is defined by the MRS of TR 5. The TR 6 sequence is 30 m thick in borehole DH2 and occurs in the middle to upper part of the Slottsmøya Member. Core data in DH2, with a lower FU passing upward to two CU units together with the dimactite in DH5R which can be used as evidence of distal response to a prograding coastline, provide the basis for the defined TR 6. Due to proximity to the decollement zone in the uppermost part of the formation in DH5R (Fig. 17), the TR sequence is here probably incomplete. TR 6 ends our proposed T–R subdivision of the Agardhfjellet Formation in central western Spitsbergen.

Age: Middle Volgian to Ryazanian, including the *Taimyrensis* zone. Ryazanian deposits are directly recognised in our cores only by the single find of the earliest Ryazanian ammonite *Chetaites sibiricus* at 507 m in borehole DH2, but Late Ryazanian and possibly Early Ryazanian ammonites were found in hydrocarbon seep carbonates in the Janusfjellet area by Wierzbowski et al. (2011).

Sedimentological expression: In the lower part, TR 6 fines upwards from silty shale F2 or heterolithic sandstone F3 to blocky paper shale; F1. The regressive part in borehole DH5R is passing upward to a c. 20 m-thick diamictite, F5. As in TR 5, the upper part of TR 6 in both DH2 and DH5R consists of a mixture of facies associations FA 1, 2 and 3.

Sequence-stratigraphic expression of the surfaces: As in TR 3, the MRS of TR 6 is placed close to the boundary between the Volgian and the Ryazanian which might have a small hiatus. The MFS is placed in the middle part of the first black paper shale accompanied by an increase in TOC and above the diamictite in borehole DH5R. Also, we speculate that the slumped deposits might mark the sudden onset of regression, e.g., from a slump scar due to unstable clay sediments.

Summary and conclusions

The frost weathering in the Arctic, the dominant shale lithology and diagenesis (Dypvik, 1984b; Dypvik et al., 1991a, b; Dypvik & Zakharov, 2012) of the Agardhfjellet Formation reduce the quality of preservation of macrofossils. Invertebrate fauna preserved as moulds are destroyed easily by the frost wedging. This affects the probability of finding invertebrate fossils in the field, and as a result most ammonite finds were restricted to sideritic and carbonate beds. Many studies have been performed on these ammonites by e.g., Rogov (2010, 2014), Rogov & Mironenko (2016), Wierzbowski (1989) and Wierzbowski et al. (2011). The ammonite zones derived from this work fit very well with our finds in the shale parts of the cores, except for the fact

that Oxfordian ammonites are relatively rare in Central Spitsbergen (Parker, 1967; Rogov, 2014; Koevoets et al., 2016). Koevoets et al. (2016) identified an Oxfordian *Cardioceras* in the Oppdalen Member (at 705 m) in borehole DH2. The ammonites used in this study place the Oppdalen Member in the Bathonian to Lower Oxfordian with the presence of *Kepplerites* (*S.*) *svalbardensis* and *Cardioceras* sp.. The Lardyfjellet Member is believed to be Early Kimmeridgian in age, based on the presence of *Amoebites subkitchini* in the lower part and numerous ammonites of the *kitchini* Zone higher in the member. The Oppdalssåta Member with *Hoplocardioceras elegans* is considered to be mostly Upper Kimmeridgian; and finally, with the presence of *Dorsoplanites* sp., the Slottsmøya Member was deposited during the Volgian for the most part.

The cores have proven to contain a wealth of invertebrate fauna. Even so, some sections of the formation have uncertain age determinations due to the lack of ammonites. Improved age constraints on the entire formation were achieved by studies on palynomorphs (Bjærke, 1980; Århus, 1988; Dalseg et al., 2016b). Palynomorphs in the Agardhfjellet Formation are not well preserved, but some conclusions could still be made from the rough sampling here. The Bathonian – Lower Callovian is situated in the lower Oppdalen Member, as confirmed by the first appearance of *Sirmiodinium grossii* and the last appearance of *Valvaeodinium spinosum*. The Oppdalssåta Member is believed to be roughly Late Kimmeridgian in age with the presence of *Atopodinium haromense*, *Cribroperidinium* sp. and *Rhyncodiniopsis cladophora,* while the Slottsmøya Member falls into the Volgian to Ryazanian age range. The palynology fits well with the ammonite age determinations. The age control on the strata is therefore considered to be well established and the formation ranges from Bathonian to the Ryazanian–Valanginian boundary (age c. 140 Ma–167 Ma; Fig. 16).

The wireline log and TOC curve in Figs. 4 & 5 show a strong peak in organic material/kerogen in the Lardyfjellet Member. The depositional environment and specifically the oxygenation of the deposited sediments seem to vary greatly throughout the formation. As shown in Fig. 6, about 80% of the XRF-scanned samples indicate an anoxic depositional environment and 20% fall within the dysoxic range. Black shales and glauconitic deposits are associated with reducing conditions (Wignall, 1994; Stonecipher, 1999). V/(V + Ni) shows the highest levels of anoxia in the Oppdalen Member and Lardyfjellet Member and the top of the Slottsmøya Member (including the Myklegardfjellet Bed), which is consistent with the interpretation of these sections as outer shelf mud deposits (FA 1) and offshore condensed marine deposits (FA 2). In the Oppdalssåta Member and Slottsmøya Member, the oxygenation shows more alternation between dysoxia and anoxia. This is consistent with the more common occurrence of sandstone and siltstone beds, heterolithics, of a transition zone/prodelta (FA 3) or shoreface/delta front (FA 4).

Based on six defined TR sequences, we have interpreted the Agardhfjellet Formation as a distal response to progradation and retrogradation of a coastline. Back-stepping of the coastline in the Bathonian to Early Oxfordian (TR 1) may have been followed by a middle to upper Oxfordian hiatus in central Spitsbergen, although ammonites of this age have been found in western and southern Spitsbergen and at Kong Karls Land (e.g., Kopik & Wierzbowski, 1988). The next two TR sequences (TR 2 and TR 3), with distal delta-front or lower middle shoreface deposits in the upper parts of their CU units, reflect forward stepping of the coastline in the Kimmeridgian to earliest Volgian. The Lower Volgian to Ryazanian TR sequences, TR 5 and 6, have much more distal facies in the upper part of each CU unit suggesting a retreat of the coastline compared with the Kimmeridgian to lowermost Volgian sequences. The Lower Volgian TR 4 is then interpreted as the turning point of a large-scale lower Kimmeridgian to Ryazanian prograding and retrograding clastic wedge.

The lower sequence TR 1, with its sequence boundary at the top of the Brentskardhaugen Bed, marks a dramatic shift from coarse-grained to more mud-dominated units and probably with a change in dominance of provenance area towards the west (Bue & Andresen, 2014). We propose a western/northwestern provenance for the sediments which is consistent with the reconstruction of Dypvik (1984a) and Dypvik et al. (1991a, 2002), and the palaeogeographic map published by Smelror et al. (2009).

Acknowledgements. We are most grateful to Geir Elvebakk and Mikhail Rogov for their thorough reviews and constructive comments on the manuscript. This study is part of the Industry and Research Council of Norway (the Climit program) sponsored Longyearbyen CO_2 lab project (http://co2-ccs.unis.no). In addition, it is part of the 'Facies variations of Upper Jurassic source rock interval in the Barents Sea' project funded by ConocoPhillips and Lundin Norway, the ARCEx project (Research Centre for Arctic Petroleum Exploration) funded by the Industry and Research Council of Norway (grant number 228107) and the industry-sponsored JuLoCrA project led by the University of Stavanger and UNIS.

References

Abay, T.B., Karlsen, D.A., Lerch, B., Olaussen, S., Pedersen, J.H. & Backer-Owe, K. 2017: Migrated petroleum in outcropping Mesozoic sedimentary rocks in Spitsbergen: Organic geochemical characterization and implications for regional exploration. *Journal of Petroleum Geology 40*, 5–36. https://doi.org/10.1111/jpg.12662.

Amorosi, A. 1995: Glaucony and sequence stratigraphy: a conceptual framework of distribution in siliciclastic sequences. *Journal of Sedimentary Research 65*, 419–425.

Amorosi, A. 1997: Detecting compositional, spatial, and temporal attributes of glaucony: a tool for provenance research. *Sedimentary Geology 109*, 135–153. https://doi.org/10.1016/S0037-0738(96)00042-5.

Amorosi, A., Guidi, R., Mas, R. & Falanga, E. 2012: Glaucony from the Cretaceous of the Sierra de Guadarrama (Central Spain) and its application in a sequence-stratigraphic context. *International Journal of Earth Sciences 101*, 415–427. https://doi.org/10.1007/s00531-011-0675-x.

Anell, I., Braathen, A. & Olaussen, S. 2014: The Triassic - Early Jurassic of the northern Barents Shelf: a regional understanding of the Longyearbyen CO_2 reservoir. *Norwegian Journal of Geology 94*, 83–98.

Arthur, M.A. & Sageman, B.B. 1994: Marine black shales: depositional mechanisms and environments of ancient deposits. *Annual Review of Earth and Planetary Sciences 22*, 499–551. https://doi.org/10.1146/annurev.ea.22.050194.002435.

Bäckström, S.A. & Nagy, J. 1985: Depositional history and fauna of a Jurassic phosphorite conglomerate (the Brentskardhaugen Bed) in Spitsbergen. *Norsk Polarinstitutt Skrifter 183*, 1–61.

Basov, V.A., Pchelina, T.M., Vasilenko, L.K.V., Korchinskaya, M.V. & Fefilova, L.A. 1997: Substantiation of age of Mesozoic sequence boundaries on the Barents Sea shelf. *Stratigraphy and paleontology of the Russian Arctic, collection of scientific papers*, 35–48. VNIIOkeangeologia, Sankt Petersburg (in Russian).

Bergh, S.G., Braathen, A. & Andresen, A. 1997: Interaction of basement-involved and thin-skinned tectonism in the Tertiary fold-thrust belt of central Spitsbergen, Svalbard. *American Association of Petroleum Geologists Bulletin 81*, 637–661.

Birkenmajer, K. 1980: Jurassic-Lower Cretaceous succession at Agardhbukta, east Spitsbergen. *Studia Geologica Polonica 66*, 35–52.

Birkenmajer, K., Pugaczewska, H. & Wierzbowski, A. 1982: The Janusfjellet Formation (Jurassic-Lower Cretaceous) at Myklegardfjellet, East Spitsbergen. *Palaeontologia Polonica 43*, 107–140.

Bjærke, T. 1980: Mesozoic palynology of Svalbard V. Dinoflagellates from the Agardhfjellet Member (Middle and Upper Jurassic) in Spitsbergen. *Norsk Polarinstitutt Skrifter 172*, 145–167.

Braathen, A., Bergh, S.G. & Maher, H.D. 1995: Structural outline of a Tertiary basement-cored uplift inversion structure in western Spitshergen, Svalbard-kinematics and controlling factors. *Tectonics 14*, 95–119. https://doi.org/10.1029/94TC01677.

Braathen, A., Bælum, K., Christiansen, H.H., Dahl, T., Eiken, O., Elvebakk, H., Hansen, F., Hanssen, T.H., Jochmann, M., Johansen, T.A., Johnsen, H., Larsen, L., Lie, T., Mertes, J., Mørk, A., Mørk, M.B., Nemec, W., Olaussen, S., Oye, V., Rød, K., Titlestad, G.O., Tveranger, J. & Vagle, K. 2012: The Longyearbyen CO_2 Lab of Svalbard, Norway-initial assessment of the geological conditions for CO_2 sequestration. *Norwegian Journal of Geology 92*, 353–376.

Brekke, T., Krajewski, K.P. & Hubred, J.H. 2014: Organic geochemistry and petrography of thermally altered sections of the Middle Triassic Botneheia Formation on south-western Edgeøya, Svalbard. *Norwegian Petroleum Directorate Bulletin 11*, 111–128.

Bue, E.P. & Andresen, A. 2014: Constraining depositional models in the Barents Sea region using detrital zircon U–Pb data from Mesozoic sediments in Svalbard. *Geological Society of London Special Publications 386*, 261–279. https://doi.org/10.1144/SP386.14.

Collignon, M. & Hammer, Ø. 2012: Petrography and sedimentology of the Slottsmøya Member at Janusfjellet, central Spitsbergen. *Norwegian Journal of Geology 92*, 89–101.

Dallmann, W.K. (ed.) 1999: Lithostratigraphic Lexicon of Svalbard. Norsk Polarinstitutt, Tromsø, 318 pp.

Dallmann, W.K., Kjærnet, T. & Nøttvedt, A. 2001: Geological map of Svalbard 1:100,000, sheet C9G Adventdalen. Map description, 1–55.

Dalseg, T.S., Nakrem, H.A. & Smelror, M. 2016a: Organic-walled microfossils and palynodebris in cold seep carbonate deposits: The Upper Jurassic–Lower Cretaceous Agardhfjellet Formation on Svalbard (Arctic Norway). *Norwegian Journal of Geology 96*, 135–146. https://doi.org/10.17850/njg96-2-01.

Dalseg, T.S., Nakrem, H.A. & Smelror, M. 2016b: Dinoflagellate biostratigraphy, palynofacies, depositional environment and sequence stratigraphy of the Agardhfjellet Formation (Upper Jurassic–Lower Cretaceous) in central Spitsbergen (Arctic Norway). *Norwegian Journal of Geology 96*, 119–133. https://doi.org/10.17850/njg96-2-04.

Delsett, L.L., Novis, L.K., Roberts, A.J., Koevoets, M.J., Hammer, Ø., Druckenmiller, P.S. & Hurum, J.H. 2016: The Slottsmøya marine reptile Lagerstätte: depositional environments, taphonomy and diagenesis. *Geological Society of London Special Publications 434*, 165–188. https://doi.org/10.1144/SP434.2.

Delsett, L.L., Roberts, A.J., Druckenmiller, P.S. & Hurum, J.H. 2017: A new ophthalmosaurid (Ichthyosauria) from Svalbard, Norway, and evolution of the ichthyopterygian pelvic girdle. *PloS one 12*, e0169971. https://doi.org/10.1371/journal.pone.0169971.

Druckenmiller, P.S., Hurum, J.H., Knutsen, E.M. & Nakrem, H.A. 2012: Two new ophthalmosaurids (Reptilia: Ichthyosauria) from the Agardhfjellet Formation (Upper Jurassic: Volgian/Tithonian), Svalbard, Norway. *Norwegian Journal of Geology 92*, 311–339.

Dumas, S. & Arnott, R. 2006: Origin of hummocky and swaley cross-stratification—the controlling influence of unidirectional current strength and aggradation rate. *Geology 34*, 1073–1076. https://doi.org/10.1130/G22930A.1.

Dypvik, H. 1984a: Geochemical compositions and depositional conditions of Upper Jurassic and Lower Cretaceous Yorkshire clays, England. *Geological Magazine 121*, 489–504. https://doi.org/10.1017/S0016756800030028.

Dypvik, H. 1984b: Jurassic and Cretaceous black shales of the Janusfjellet Formation, Svalbard, Norway. *Sedimentary Geology 41*, 235–248. https://doi.org/10.1016/0037-0738(84)90064-2.

Dypvik, H. & Harris, N.B. 2001: Geochemical facies analysis of fine-grained siliciclastics using Th/U, Zr/Rb and (Zr+Rb)/Sr ratios. *Chemical Geology 181*, 131–146. https://doi.org/10.1016/S0009-2541(01)00278-9.

Dypvik, H. & Zakharov, V. 2012: Fine-grained epicontinental Arctic sedimentation–mineralogy and geochemistry of shales from the Late Jurassic-Early Cretaceous transition. *Norwegian Journal of Geology 92*, 65–87.

Dypvik, H., Nagy, J., Eikeland, T.A., Backer-Owe, K., Andresen, A., Haremo, P., Bjærke, T., Johansen, H. & Elverhøi, A. 1991a: The Janusfjellet subgroup (Bathonian to Hauterivian) on central Spitsbergen - a revised lithostratigraphy. *Polar Research 9*, 21–43. https://doi.org/10.3402/polar.v9i1.6777.

Dypvik, H., Nagy, J., Eikeland, T.A., Backer-Owe, K. & Johansen, H. 1991b: Depositional conditions of the Bathonian to Hauterivian Janusfjellet Subgroup, Spitsbergen. *Sedimentary Geology 72*, 55–78. https://doi.org/10.1016/0037-0738(91)90123-U.

Dypvik, H., Nagy, J. & Krinsley, D.H. 1992: Origin of the Myklegardfjellet Bed, a basal Cretaceous marker on Spitsbergen. *Polar Research 11*, 21–31. https://doi.org/10.3402/polar.v11i1.6714.

Dypvik, H., Hakansson, E. & Heinberg, C. 2002: Jurassic and Cretaceous palaeogeography and stratigraphic comparisons in the North Greenland-Svalbard region. *Polar Research 21*, 91–108. https://doi.org/10.3402/polar.v21i1.6476.

Eldholm, O., Faleide, J.I. & Myhre, A.M. 1987: Continent-ocean transition at the western Barents Sea Svalbard continental margin. *Geology 15*, 1118–1122. https://doi.org/10.1130/0091-7613(1987)15<1118:CTATWB>2.0.CO;2.

Embry, A. 1993: Transgressive–regressive (T–R) sequence analysis of the Jurassic succession of the Sverdrup Basin, Canadian Arctic Archipelago. *Canadian Journal of Earth Sciences 30*, 301–320. https://doi.org/10.1139/e93-024.

Embry, A.F. 1995: Sequence boundaries and sequence hierarchies: problems and proposals. *Norwegian Petroleum Society Special Publications 5*, 1–11. https://doi.org/10.1016/S0928-8937(06)80059-7.

Embry, A. & Johannessen, E. 1993: T–R sequence stratigraphy, facies analysis and reservoir distribution in the uppermost Triassic–Lower Jurassic succession, Western Sverdrup Basin, Arctic Canada. *Arctic Geology and Petroleum Potential Special Publication 2*, 121–146. https://doi.org/10.1016/B978-0-444-88943-0.50013-7.

Faleide, J.I., Vagnes, E. & Gudlaugsson, S.T. 1993: Late Mesozoic-Cenozoic evolution of the South-Western Barents Sea in a regional rift shear tectonic setting. *Marine and Petroleum Geology 10,* 186–214. https://doi.org/10.1016/0264-8172(93)90104-Z.

Faleide, J.I., Tsikalas, F., Breivik, A.J., Mjelde, R., Ritzmann, O., Engen, O., Wilson, J. & Eldholm, O. 2008: Structure and evolution of the continental margin off Norway and the Barents Sea. *Episodes 31*, 82–91.

Frey, R.W., Pemberton, S.G. & Saunders, T.D. 1990: Ichnofacies and bathymetry: a passive relationship. *Journal of Paleontology 64*, 155–158. https://doi.org/10.1017/S0022336000042372.

Galloway, W.E. 1989: Genetic stratigraphic sequences in basin analysis I: architecture and genesis of flooding-surface bounded depositional units. *American Association of Petroleum Geologists Bulletin 73*, 125–142.

Galloway, W.E. & Hobday, D.K. 2012: *Terrigenous clastic depositional systems: Applications to fossil fuel and groundwater resources*. Springer Science & Business Media, Berlin, 491 pp.

Glørstad-Clark, E., Faleide, J.I., Lundschien, B.A. & Nystuen, J.P. 2010: Triassic seismic sequence stratigraphy and paleogeography of the western Barents Sea area. *Marine and Petroleum Geology 27*, 1448–1475. https://doi.org/10.1016/j.marpetgeo.2010.02.008.

Gradstein, F.M., Ogg, J.G., Schmitz, M. & Ogg, G. 2012: *The Geologic Time Scale 2012*. Elsevier, Amsterdam, 1176 pp.

Grundvåg, S.-A., Marin, D., Kairanov, B., Śliwińska, K.K., Nøhr-Hansen, H., Jelby, M.J., Escalona, A. & Olaussen S. 2017: The Lower Cretaceous succession of the northwestern Barents Shelf: Onshore and offshore correlation. *Marine and Petroleum Geology 86*, 834-857.

Hammer, Ø., Nakrem, H.A., Little, C.T.S., Hryniewicz, K., Sandy, M.R., Hurum, J.H., Druckenmiller, P.S., Knutsen, E.M. & Høyberget, M. 2011: Hydrocarbon seeps from close to the Jurassic–Cretaceous boundary, Svalbard. *Palaeogeography, Palaeoclimatology, Palaeoecology 306*, 15–26. https://doi.org/10.1016/j.palaeo.2011.03.019.

Hammer, Ø., Collignon, M. & Nakrem, H.A. 2012: Organic carbon isotope chemostratigraphy and cyclostratigraphy in the Volgian of Svalbard. *Norwegian Journal of Geology 92*, 103–112.

Hammer, Ø., Hryniewicz, K., Hurum, J.H., Høyberget, M., Knutsen, E.M. & Nakrem, H.A. 2013: Large onychites (cephalopod hooks) from the Upper Jurassic of the Boreal Realm. *Acta Palaeontologica Polonica 58*, 827–835.

Harland, W.B., Anderson, L.M., Manasrah, D., Butterfield, N.J., Challinor, A., Doubleday, P.A., Dowdeswell, E.K., Dowdeswell, J.A., Geddes, I., Kelly, S.R.A., Lesk, E.L., Spencer, A.M. & Stephens, C.F. 1997: *The geology of Svalbard*. Geological Society of London Memoirs 17, Geological Society of London, 521 pp.

Hatch, J.R. & Leventhal, J.S. 1992: Relationship between inferred redox potential of the depositional environment and geochemistry of the Upper Pennsylvanian (Missourian) Stark Shale Member of the Dennis Limestone, Wabaunsee County, Kansas, U.S.A. *Chemical Geology 99*, 65–82. https://doi.org/10.1016/0009-2541(92)90031-Y.

Helland-Hansen, W. & Hampson, G.J. 2009: Trajectory analysis: Concepts and applications. *Basin Research 21*, 454–483. https://doi.org/10.1111/j.1365-2117.2009.00425.x.

Henriksen, E., Bjørnseth, H.M., Hals, T.K., Heide, T., Kiryukhina, T., Kløvjan, O.S., Larssen, G.B., Ryseth, A.E., Rønning, K., Sollid, K. & Stoupakova, A. 2011: Uplift and erosion of the greater Barents Sea: impact on prospectivity and petroleum systems. *Geological Society of London Memoirs 35*, 271–281.

Holmer, L.E. & Nakrem, H.A. 2012: The lingulid brachiopod *Lingularia* from lowermost Cretaceous hydrocarbon seep bodies, Sassenfjorden area, central Spitsbergen, Svalbard. *Norwegian Journal of Geology 92*, 167–174.

Howard, J.D. & Reineck, H.E. 1981: Depositional facies of high-energy beach-to- offshore sequence: comparison with low-energy sequence. *American Association of Petroleum Geologists Bulletin 65*, 807–830.

Hryniewicz, K., Hammer, Ø., Nakrem, H.A. & Little, C.T.S. 2012: Microfacies of the Volgian-Ryazanian (Jurassic-Cretaceous) hydrocarbon seep carbonates from Sassenfjorden, central Spitsbergen, Svalbard. *Norwegian Journal of Geology 92*, 113–131.

Hryniewicz, K., Little, C.T.S. & Nakrem, H.A. 2014: Bivalves from the latest Jurassic-earliest Cretaceous hydrocarbon seep carbonates from central Spitsbergen, Svalbard. *Zootaxa 3859*, 1–66. https://doi.org/10.11646/zootaxa.3859.1.1.

Hryniewicz, K., Nakrem, H.A., Hammer, Ø., Little, C.T.S., Kaim, A., Sandy, M.R. & Hurum, J.H. 2015: The palaeoecology of the latest Jurassic – earliest Cretaceous hydrocarbon seep carbonates from Spitsbergen, Svalbard. *Lethaia 48*, 353–374. https://doi.org/10.1111/let.12112.

Hurum, J.H., Nakrem, H.A., Hammer, Ø., Knutsen, E.M., Druckenmiller, P.S., Hryniewicz, K. & Novis, L.K. 2012: An Arctic Lagerstätte - the Slottsmøya Member of the Agardhfjellet Formation (Upper Jurassic-Lower Cretaceous) of Spitsbergen. *Norwegian Journal of Geology 92*, 55–64.

Hvoslef, S., Dypvik, H. & Solli, H. 1986: A combined sedimentological and organic geochemical study of the Jurassic/Cretaceous Janusfjellet Formation (Svalbard), Norway. *Organic Geochemistry 10*, 101–111. https://doi.org/10.1016/0146-6380(86)90013-6.

Høy, T. & Lundschien, B.A. 2011: Triassic deltaic sequences in the northern Barents Sea. *Geological Society of London Memoirs 35*, 249–260.

Ilyina, V.I., Nikitenko, B.L. & Glinskikh, L.A. 2005: Foraminifera and dinoflagellate cyst zonation and stratigraphy of the Callovian to Volgian reference section in the Tyumenskaya superdeep well (West Siberia, Russia). *In* Powell, A.J. & Riding, J.B. (eds.): *Recent Developments in Applied Biostratigraphy*, The Micropalaeontological Society Special Publications, Geological Society og London, Bath, pp. 109–147.

Jones, B. & Manning, D.A.C. 1994: Comparison of geochemical indices used for the interpretation of palaeoredox conditions in ancient mudstones. *Chemical Geology 111*, 111–129. https://doi.org/10.1016/0009-2541(94)90085-X.

Jones, M.T., Augland, L.E., Shephard, G.E., Burgess, S.D., Aliassen, G.T., Jochmann, M.M., Friis, B., Jerram, D.A., Planke, S. & Svensen, H.H. 2017. Constraining shifts in North Atlantic plate motions during the Palaeocene by U-Pb dating of Svalbard tephra layers. *Scientific Reports 7*, 6822, 9 pp. https://doi.org/10.1038/s41598-017-06170-7.

Katz, M.E., Wright, J.D., Miller, K.G., Cramer, B.S., Fennel, K. & Falkowski, P.G. 2005: Biological overprint of the geological carbon cycle. *Marine Geology 217*, 323–338. https://doi.org/10.1016/j.margeo.2004.08.005.

Klausen, T.G., Ryseth, A.E., Helland-Hansen, W., Gawthorpe, R. & Laursen, I. 2015: Regional development and sequence stratigraphy of the Middle to Late Triassic Snadd Formation, Norwegian Barents Sea. *Marine and Petroleum Geology 62*, 102–122. https://doi.org/10.1016/j.marpetgeo.2015.02.004.

Knaust, D. 2015: Siphonichnidae (new ichnofamily) attributed to the burrowing activity of bivalves: ichnotaxonomy, behaviour and palaeoenvironmental implications. *Earth-Science Reviews 150*, 497–519. https://doi.org/10.1016/j.earscirev.2015.07.014.

Knaust, D. 2017: *Atlas of Trace Fossils in Well Core: Appearance, Taxonomy and Interpretation*. Springer, Dordrecht, xv + 209 pp.

Knaust, D. & Bromley, R.G. 2012: *Trace Fossils as Indicators of Sedimentary Environments*. Developments in Sedimentology 64, Elsevier, Oxford, xxx + 960 pp.

Knutsen, E.M., Druckenmiller, P.S. & Hurum, J.H. 2012: Two new species of long-necked plesiosaurians (Reptilia: Sauropterygia) from the Upper Jurassic (Middle Volgian) Agardhfjellet Formation of central Spitsbergen. *Norwegian Journal of Geology 92*, 187–212.

Koevoets, M.J., Abay, T.B., Hammer, Ø. & Olaussen, S. 2016: High-resolution organic carbon–isotope stratigraphy of the Middle Jurassic–Lower Cretaceous Agardhfjellet Formation of central Spitsbergen, Svalbard. *Palaeogeography, Palaeoclimatology, Palaeoecology 449*, 266–274. https://doi.org/10.1016/j.palaeo.2016.02.029.

Kopik, J. & Wierzbowski, A. 1988: Ammonites and stratigraphy of the Bathonian and Callovian at Janusfjellet and Wimanfjellet, Sassenfjorden, Spitsbergen, Norway. *Acta Palaeontologica Polonica 33*, 145–168.

Krajewski, K. 1990: Phosphoritization in a starved shallow shelf environment: the Brentskardhaugen Bed (Toarcian-Bajocian) in Spitsbergen. *Polish Polar Research 11*, 331–344.

Krajewski, K.P. 2004: Carbon and oxygen isotopic survey of diagenetic carbonate deposits in the Agardhfjellet Formation (Upper Jurassic), Spitsbergen: Preliminary results. *Polish Polar Research 25*, 27–43.

Krajewski, K.P., Lacka, B., Kuzniarski, M., Orlowski, R. & Prejbisz, A. 2001. Diagenetic origin of carbonate in the Marhøgda Bed (Jurassic) in Spitsbergen, Svalbard. *Polish Polar Research 22*, 89–128.

Kylander, M.E., Ampel, L., Wohlfarth, B. & Veres, D. 2011: High-resolution X-ray fluorescence core scanning analysis of Les Echets (France) sedimentary sequence: New insights from chemical proxies. *Journal of Quaternary Science 26*, 109–117. https://doi.org/10.1002/jqs.1438.

Leever, K.A., Gabrielsen, R.H., Faleide, J.I. & Braathen, A. 2011: A transpressional origin for the West Spitsbergen fold-and-thrust belt: Insight from analog modeling. *Tectonics 30*, TC2014, 24 pp. https://doi.org/10.1029/2010TC002753.

Loutit, T.S., Hardenbol, J., Vail, P.R. & Baum, G.R. 1988: Condensed sections: the key to age determination and correlation of continental margin sequences. *Society for Sedimentary Geology Special Publication 42*, 183–213. https://doi.org/10.2110/pec.88.01.0183.

Macquaker, J. & Gawthorpe, R. 1993: Mudstone lithofacies in the Kimmeridge Clay Formation, Wessex Basin, southern England: implications for the origin and controls of the distribution of mudstones. *Journal of Sedimentary Petrology 63*, 1129–1143.

Macquaker, J.H., Bentley, S.J. & Bohacs, K.M. 2010: Wave-enhanced sediment-gravity flows and mud dispersal across continental shelves: Reappraising sediment transport processes operating in ancient mudstone successions. *Geology 38*, 947–950. https://doi.org/10.1130/G31093.1.

Maher, H.D. 2001: Manifestations of the Cretaceous High Arctic Large Igneous Province in Svalbard. *Journal of Geology 109*, 91–104. https://doi.org/10.1086/317960.

Marshall, C., Uguna, J., Large, D.J., Meredith, W., Jochmann, M., Friis, B., Vane, C., Spiro, B.F., Snape, C.E. & Orheim, A. 2015: Geochemistry and petrology of Palaeocene coals from Spitzbergen Part 2: Maturity variations and implications for local and regional burial models. *International Journal of Coal Geology 143*, 1–10. https://doi.org/10.1016/j.coal.2015.03.013.

Midtkandal, I., Svensen, H., Planke, S., Corfu, F., Polteau, S., Torsvik, T.H., Faleide, J.I., Grundvåg, S.-A., Selnes, H. & Olaussen, S. 2016. The Aptian oceanic anoxic event (OAE1a) in Svalbard and the age of the Barremian-Aptian boundary. *Palaeogeography, Palaeoclimatology, Palaeoecology 463*, 126–135. https://doi.org/10.1016/j.palaeo.2016.09.023.

Minakov, A., Mjelde, R., Faleide, J.I., Flueh, E.R., Dannowski, A. & Keers, H. 2012: Mafic intrusions east of Svalbard imaged by active-source seismic tomography. *Tectonophysics 518–521*, 106–118. https://doi.org/10.1016/j.tecto.2011.11.015.

Mulder, T. & Alexander, J. 2001: The physical character of subaqueous sedimentary density flows and their deposits. *Sedimentology 48*, 269–299. https://doi.org/10.1046/j.1365-3091.2001.00360.x.

Mulder, T., Syvitski, J.P.M., Migeon, S., Faugères, J.C. & Savoye, B. 2003: Marine hyperpycnal flows: Initiation, behaviorand related deposits. A review. *Marine and Petroleum Geology 20*, 861–882. https://doi.org/10.1016/j.marpetgeo.2003.01.003.

Mørk, A., Dallmann, W.K., Dypvik, H., Johannessen, E.P., Larssen, G.B., Nagy, J., Nøttvedt, A., Olaussen, S., Pčelina, T.M. & Worsley, D. 1999: Mesozoic lithostratigraphy. *In* Dallmann, W.K. (ed.): *Lithostratigraphic lexicon of Svalbard. Review and recommendations for nomenclature use. Upper Palaeozoic to Quaternary bedrock*, Norsk Polarinstitutt, Tromsø, Norway, pp. 127–214.

Nagy, J. & Basov, V.A. 1998: Revised foraminiferal taxa and biostratigraphy of Bathonian to Ryazanian deposits in Spitsbergen. *Micropaleontology 44*, 217–255. https://doi.org/10.2307/1486047.

Nagy, J., Löfaldli, M., Bäckström, S.A. & Johansen, H. 1990: Agglutinated foraminiferal stratigraphy of Middle Jurassic to basal Cretaceous shales, Central Spitsbergen. *In* Hemleben, C., Kaminski, M.A., Kuhnt, W. & Scott, D.B. (eds.): *Paleoecology, Biostratigraphy, Paleoceanography and Taxonomy of Agglutinated Foraminifera.* Springer Netherlands, Dordrecht, pp. 969–1015. https://doi.org/10.1007/978-94-011-3350-0_38.

Nagy, J., Reolid, M. & Rodriguez-Tovar, F.J. 2009: Foraminiferal morphogroups in dysoxic shelf deposits from the Jurassic of Spitsbergen. *Polar Research 28*, 214–221. https://doi.org/10.1111/j.1751-8369.2009.00112.x.

Nichols, G. 2009: *Sedimentology and stratigraphy*. John Wiley & Sons, Hoboken, 419 pp.

Nunn, E.V., Price, G.D., Hart, M.B., Page, K.N. & Leng, M.J. 2009: Isotopic signals from Callovian-Kimmeridgian (Middle-Upper Jurassic) belemnites and bulk organic carbon, Staffin Bay, Isle of Skye, Scotland. *Journal of the Geological Society of London 166*, 633–641. https://doi.org/10.1144/0016-76492008-067.

Odin, G.S. & Matter, A. 1981: De glauconiarum origine. *Sedimentology 28*, 611–641. https://doi.org/10.1111/j.1365-3091.1981.tb01925.x.

Ogata, K., Senger, K., Braathen, A., Tveranger, J. & Olaussen, S. 2012: The importance of natural fractures in a tight reservoir for potential CO_2 storage: a case study of the upper Triassic–middle Jurassic Kapp Toscana Group (Spitsbergen, Arctic Norway). *In* Spence, G.H., Redfern, J., Aguilera, R., Bevan, T.G., Cosgrove, J.W., Couples, G.D. & Daniel, J.M. (eds.): *Advances in the Study of Fractured Reservoirs*, Geological Society of London Special Publications 374, pp. 395–415.

Parker, J.R. 1967: The Jurassic and Cretaceous sequence in Spitsbergen. *Geological Magazine 104*, 487–505. https://doi.org/10.1017/S0016756800049220.

Parsons, J.D., Bush, J.W. & Syvitski, J.P. 2001: Hyperpycnal plume formation from riverine outflows with small sediment concentrations. *Sedimentology 48*, 465–478. https://doi.org/10.1046/j.1365-3091.2001.00384.x.

Passey, Q.R., Creaney, S., Kulla, J.B., Moretti, F.J. & Stroud, J.D. 1990: A practical model for organic richness from porosity and resistivity logs. *American Association of Petroleum Geologists Bulletin 74*, 1777–1794.

Peters, S.E. & Loss, D.P. 2012. Storm and fair-weather wave base: A relevant distinction? *Geology 40*, 511–514. https://doi.org/10.1130/G32791.1.

Podlaha, O.G., Mutterlose, J. & Veizer, J. 1998: Preservation of $\delta^{18}O$ and $\delta^{13}C$ in belemnite rostra from the Jurassic/Early Cretaceous successions. *American Journal of Science 298*, 324–347. https://doi.org/10.2475/ajs.298.4.324.

Poulsen, N.E. & Riding, J.B. 2003: The Jurassic dinoflagellate cyst zonation of subboreal Northwest Europe. *Geological Survey of Denmark and Greenland Bulletin 1*, 115–144.

Powell, W.G., Johnston, P.A. & Collom, C.J. 2003: Geochemical evidence for oxygenated bottom waters during deposition of fossiliferous strata of the Burgess Shale Formation. *Palaeogeography, Palaeoclimatology, Palaeoecology 201*, 249–268. https://doi.org/10.1016/S0031-0182(03)00612-6.

Pratt, T.L., Hauser, E.C. & Nelson, K.D. 1992: Widespread buried Precambrian layered sequences in the U.S. mid- continent: evidence for large Proterozoic depositional basins. *American Association of Petroleum Geologists Bulletin 76*, 1384–1401.

Price, G.D. & Rogov, M.A. 2009: An isotopic appraisal of the Late Jurassic greenhouse phase in the Russian Platform. *Palaeogeography, Palaeoclimatology, Palaeoecology 273*, 41–49. https://doi.org/10.1016/j.palaeo.2008.11.011.

Riding, J.B. & Thomas, J.E. 1992: Dinoflagellate cysts of the Jurassic System. *In* A.J. Powell (ed.): *A stratigraphic index of dinoflagellate cysts*, Springer, Berlin, pp. 7–97. https://doi.org/10.1007/978-94-011-2386-0_2.

Riis, F., Lundschien, B.A., Høy, T., Mørk, A. & Mørk, M.B.E. 2008: Evolution of the Triassic shelf in the northern Barents Sea region. *Polar Research 27*, 318–338. https://doi.org/10.1111/j.1751-8369.2008.00086.x.

Rismyhr, B. Bjærke, T., Olaussen, S., Mulrooney, M. J. & Senger K. In press. Facies, palynostratigraphy and sequence stratigraphy of the Wilhelmøya Subgroup (Upper Triassic–Middle Jurassic) in western central Spitsbergen, Svalbard. *Norwegian Journal of Geology.*

Rogov, M.A. 2010: New data on ammonites and stratigraphy of the Volgian stage in Spitzbergen. *Stratigraphy and Geological Correlation 18*, 505–531. https://doi.org/10.1134/S0869593810050047.

Rogov, M.A. 2014: An infrazonal ammonite biostratigraphy for the Kimmeridgian of Spitsbergen. *Norwegian Petroleum Directorate Bulletin 11*, 153–165.

Rogov, M.A. & Mironenko, A. 2016: Patterns of the evolution of aptychi of Middle Jurassic to Early Cretaceous Boreal ammonites. *Swiss Journal of Palaeontology 135*, 139–151. https://doi.org/10.1007/s13358-015-0110-1.

Rousseau, J. & Nakrem, H.A. 2012: An Upper Jurassic Boreal echinoderm Lagerstätte from Janusfjellet, central Spitsbergen. *Norwegian Journal of Geology 92*, 133–161.

Sand, G., Braathen, A. & Olaussen, S. 2014: Longyearbyen CO_2 Lab - tales of research and education. *Norwegian Journal of Geology 94*, 77–82.

Senger, K., Roy, S., Braathen, A., Buckley, S.J., Baelum, K., Gernigon, L., Mjelde, R., Noormets, R., Ogata, K., Olaussen, S., Planke, S., Ruud, B.O. & Tveranger, J. 2013: Geometries of doleritic intrusions in central Spitsbergen, Svalbard: an integrated study of an onshore-offshore magmatic province with implications for CO_2 sequestration. *Norwegian Journal of Geology 93*, 143–166.

Senger, K., Tveranger, J., Ogata, K., Braathen, A. & Planke, S. 2014: Late Mesozoic magmatism in Svalbard: A review. *Earth-Science Reviews 139*, 123–144. https://doi.org/10.1016/j.earscirev.2014.09.002.

Shurygin, B.N. & Dzyuba, O.S. 2015: The Jurassic-Cretaceous boundary in northern Siberia and Boreal-Tethyan correlation of the boundary beds. *Russian Geology and Geophysics 56*, 652–662. https://doi.org/10.1016/j.rgg.2015.03.013.

Smelror, M. 1988a: Late Bathonian to Early Oxfordian dinoflagellate cyst stratigraphy of Jameson Land, East Greenland. *Rapp. Grønlands geologiske Undersøgelser 137*, 135–159.

Smelror, M. 1988b: Bathonian to early Oxfordian dinoflagellate cysts and acritarchs from Kong Karls Land, Svalbard. *Review of Palaeobotany and Palynology 56*, 275–303. https://doi.org/10.1016/0034-6667(88)90061-9.

Smelror, M. & Below, R. 1992: Dinoflagellate biostratigraphy of the Toarcian to Lower Oxfordian (Jurassic) of the Barents Sea region. *Norwegian Petroleum Society Special Publication 2*, 495–513. https://doi.org/10.1016/B978-0-444-88943-0.50035-6.

Smelror, M., Mørk, A., Monteil, E., Rutledge, D. & Leereveld, H. 1998: The Klippfisk Formation - a lithostratigraphic unit of Lower Cretaceous platform carbonates on the Western Barents Shelf. *Polar Research 17*, 181–202. https://doi.org/10.1111/j.1751-8369.1998.tb00271.x.

Smelror, M., Mørk, A., Mørk, M.B.E., Weiss, H.M. & Løseth, H. 2001: Middle Jurassic-Lower Cretaceous transgressive-regressive sequences and facies distribution off northern Nordland and Troms, Norway. *Norwegian Petroleum Society Special Publications 10*, 211–232. https://doi.org/10.1016/S0928-8937(01)80015-1.

Smelror, M., Petrov, O.V., Larsen, G.B. & Werner, S. (eds.) 2009: *Atlas—Geological History of the Barents Sea*. Geological Survey of Norway, Trondheim, 135 pp.

Smirnova, T.N., Ushatinskaya, G.T., Zhegallo, E.A. & Panchenko, I.V. 2015: *Lingularia* Biernat et Emig, 1993 from the Upper Jurassic of western Siberia: Larval and embryonic shells and shell microstructure. *Paleontological Journal 49*, 125–133. https://doi.org/10.1134/S0031030115020100.

Sokolov, D. & Bodylevsky, W. 1931. Jura- und Kreidefaunen von Spitzbergen. *Skrifter om Svalbard og Ishavet 35*, 1–151.

Steel, R. & Olsen, T. 2002: Clinoforms, clinoform trajectories and deepwater sands. *Sequence-stratigraphic models for exploration and production: Evolving methodology, emerging models and application histories: Gulf Coast Section SEPM 22nd Research Conference, 8–11 December, Houston, Texas*, p. 25. https://doi.org/10.5724/gcs.02.22.0367.

Steel, R.J. & Worsley, D. 1984: Svalbard's post- Caledonian strata - an atlas of sedimentational patterns and palaeogeographic evolution. *Petroleum geology of the north European margin. Proceedings NEMS '83, Trondheim, 1983*, 109–135.

Stonecipher, S.A. 1999: Genetic characteristics of glauconite and siderite: Implications for the origin of ambiguous isolated marine sandbodies. *Society for Sedimentary Geology Special Publication 64*, 191–204. https://doi.org/10.2110/pec.99.64.0191.

Tribovillard, N., Algeo, T.J., Lyons, T. & Riboulleau, A. 2006: Trace metals as paleoredox and paleoproductivity proxies: An update. *Chemical Geology 232*, 12–32. https://doi.org/10.1016/j.chemgeo.2006.02.012.

Walker, R.G. & James, N. 1992: Facies models: response to sea level change. St. John's, Newfoundland, Geological Association of Canada, 409 pp.

Walker, K.R., Shanmugam, G. & Ruppel, S.C. 1983: A model for carbonate to terrigenous clastic sequences. *Geological Society of America Bulletin 94*, 700–712. https://doi.org/10.1130/0016-7606(1983)94<700:AMFCTT>2.0.CO;2.

Wang, S., Dong, D., Wang, Y., Li, X., Huang, J. & Guan, Q. 2016: Sedimentary geochemical proxies for paleoenvironment interpretation of organic-rich shale: A case study of the Lower Silurian Longmaxi Formation, Southern Sichuan Basin, China. *Journal of Natural Gas Science and Engineering 28*, 691–699. https://doi.org/10.1016/j.jngse.2015.11.045.

Wierzbowski, A. 1989: Ammonites and stratigraphy of the Kimmeridgian at Wimanfjellet, Sassenfjorden, Spitsbergen. *Acta Palaeontologica Polonica 34*, 355–378.

Wierzbowski, A., Hryniewicz, K., Hammer, Ø., Nakrem, H.A. & Little, C.T.S. 2011: Ammonites from hydrocarbon seep carbonate bodies from the uppermost Jurassic - lowermost Cretaceous of Spitsbergen and their biostratigraphical importance. *Neues Jahrbuch für Geologie und Paläontologie-Abhandlungen 262*, 267–288. https://doi.org/10.1127/0077-7749/2011/0198.

Wignall, P.B. 1994: *Black shales*. Oxford University Press, Oxford, 144 pp.

Worsley, D. 2008: The post-Caledonian development of Svalbard and the western Barents Sea. *Polar Research 27*, 298–317. https://doi.org/10.1111/j.1751-8369.2008.00085.x.

Zakharov, V.A., Rogov, M.A., Dzyuba, O.S., Žák, K., Košťák, M., Pruner, P., Skupien, P., Chadima, M., Mazuch, M. & Nikitenko, B.L. 2014: Palaeoenvironments and palaeoceanography changes across the Jurassic/Cretaceous boundary in the Arctic realm: case study of the Nordvik section (north Siberia, Russia). *Polar Research 33*, 19714, 19 pp.

Århus, N. 1988: Palynostratigraphy of some Bathonian–Hauterivian sections in the Arctics, with emphasis on the Janusfjellet Formation type section, Spitsbergen. *Unpublished, Institutt for kontinentalundersøkelser Report*, 1–139.